Computation of Turbulent Flows-State-of-the-Art, 1970

by

W. C. Reynolds

Prepared from work done under Grants
NSF-GK-10034 and
NASA-NgR-05-020-420

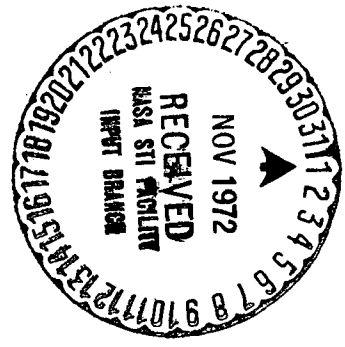

Report MD-27

Thermosciences Division
Department of Mechanical Engineering
Stanford University
Stanford, California

October 1970
(Reprinted February 1972)

COMPUTATION OF TURBULENT FLOWS-
STATE-OF-THE-ART, 1970

by

W. C. Reynolds

Prepared from work done under Grants
NSF-GK-10034 and
NASA-NgR-05-020-420

REPORT MD-27

Thermosciences Division
Department of Mechanical Engineering
Stanford University
Stanford, California

October 1970

N

Abstract

This paper surveys the state-of-the-art of turbulent flow computation. The formulations have been generalized somewhat to increase the range of their applicability, and the excitement of current debate on equation models has been brought into the review. Some new ideas on the modeling of the pressure-strain term in the Reynolds stress equations are also suggested.

The review was prepared from lecture notes drafted for an A.I.Ch.E. short course on turbulence structure (Chicago, Nov., 1970).

NOMENCLATURE

A^+	wall layer thickness parameter (4.9)
a_{ij}	structure tensor (6.11)
$\mathcal{D}$	isotropic dissipation (6.3d)
K	pressure gradient parameter (7.3)
ℓ	turbulence length scale
$\mathcal{P}$	turbulence production $-R_{ij}S_{ij}$
P_{ij}	pressure-strain tensor (8.1)
P	mean pressure
p	fluctuation pressure
Pr_T	turbulence Prandtl number (4.20)
P_o^+	pressure gradient parameter (4.10a)
Q_i	large eddy vector velocity scale
$q^2/2$	turbulence kinetic energy density
Re	Reynolds number
R_{ij}	$\overline{u_i u_j}$, "Reynolds stress tensor"
S_{ij}	mean strain rate tensor (4.2b)
t	time
u_i	fluctuation velocity vector (u,v,w)
U_i	mean velocity vector (U,V,W)
u^*	friction velocity, $\sqrt{\tau_w/\rho}$
V_o^+	transpiration parameter (4.10b)
V_{ij}	viscous terms in R_{ij} equation (6.3a),(6.5a)
x_i	cartesian coordinate vector (x,y,z)
α	molectular thermal diffusivity
α_T	turbulent thermal diffusivity
ν	molecular kinematic viscosity
ν_T	turbulent kinematic viscosity
κ	Karman constant
ρ	mass density
τ	shear stress
τ_w	wall shear stress
Θ	mean temperature
θ	fluctuation temperature
σ_{ij}	see (6.5b)
ϵ	dissipation of turbulence energy (6.4)

ACRONYMS

CHC	Champagne, Harris, and Corrsin 1970
DH	Daly and Harlow 1970
DR	Donaldson and Rosenbaum 1968
FVF	Fluctuating Velocity Field closure
MH	Mellor and Herring 1970a,b
MVF	Mean Velocity Field closure
MVFN	Newtonian MVF closure
MTE	Mean Turbulent Energy closure
MTEN	Newtonian MTE closure
MTES	Structural MTE closure
MTEN/L	MTEN closure with dynamical length scale equation
MRS	Mean Reynolds Stress closure
MRS/L	MRS closure with dynamical length scale equation
TBLPC	TBLPC 1968
TR	Tucker and Reynolds 1968

FIGURE CAPTIONS

1. Scope and Purpose of This Survey

The objective of this survey is to provide a brief but reasonably complete account of the state-of-the-art of turbulent flow computations. The review will be limited to methods that have some scientific basis, that show promise for extension to wider classes of flows, and that have been developed to the point where at least some technical information of practical use can be obtained. Emphasis will be placed on the physical assumptions rather than on the numerical techniques. The central ideas of contemporary methods will be highlighted, and we shall direct the reader to individual sources for more detailed descriptions. An effort to both relate and critique the methods has been made. A significant portion of the material covered here is not yet published elsewhere, and this material should be valuable to workers in this field.

Generators of computational schemes for turbulent flows are often most exuberant when scant data are available for comparison with their predictions. This is indeed the case for most classes of flows, with the single exception of two-dimensional steady incompressible turbulent boundary layers. In 1968 a turbulent boundary layer prediction method calibration conference (TBLPC 1968) was held at Stanford, where for the first time a large number of methods (29) were compared on a systematic basis. This comparison established the viability of prediction methods based on various closure models of the partial differential equations describing turbulent boundary layer flows. Systematic extensions of such comparisons are now in progress in several quarters, and I am indebted to several colleagues for making their unpublished work available for this review.

In other classes of flows, such as free shear layers, unsteady boundary layer flows, flows with strong boundary layer-

inviscid region interaction, with rotation, or buoyancy, separated flows, cavity flows, etc., the data available are very spotty, and our ability to evaluate such computations is therefore limited. But it does seem clear that there remains considerable room for improvement and extension of existing methods for these flows.

Finally, there is increased activity in exploration of complex differential equation models. This effort has not been very systematic. Of particular concern is the so-called pressure-strain term in the dynamical equations for the Reynolds stresses. A systematic development of what may be a better model for this term is developed here for consideration by my colleagues.

2. The Stanford Conference*

The work leading up to the 1968 TBLPC produced a volume of target boundary layer data. A committee headed by D. Coles surveyed over 100 experiments and selected 33 flows for inclusion in this volume. The data of each experiment were carefully reanalyzed, recomputed for placement in a standard form, critiques were solicited from the experimentors, and all this was documented in a tidy manner by E. Hirst and D. Coles (TBLPC-2). These data now stand as a classic base of comparison for turbulent boundary layer prediction methods. Only the hydrodynamic aspects of these layers were considered, and a corresponding standard for thermal behavior is still lacking (though the data of W. M. Kays and his associates are rapidly becoming such a collection). Moreover, the flows selected were relatively mild. Very strong pressure gradients, transpiration, roughness, rotations, and other interesting effects were not included.

Sixteen flows were selected as mandatory computations (most predictors did the others as well). Predictors were required to start these computations in a prescribed way, to use a prescribed set of free-stream conditions, to plot the results on a standard form, and to report all free-parameter adjustments. Most of the prediction programs were set up by graduate students for operation on the Stanford computer, so that by the time of the conference considerable experience with the various methods had been developed by the host group. This was very useful in preparing a paper on the morphology of the methods (Reynolds in TBLPC-1).

---

* Executive Committee: M. Morkovin, G. Sovran, D. Coles. Host Committee: S. J. Kline, E. Hirst, W. C. Reynolds. Advisory Board: F. H. Clauser, H. W. Emmons, H. W. Liepmann, J. C. Rotta, I. Tani.

The predictors sent their computations to Stanford shortly before the meeting, and we compiled them for review at the conference. Comparisons were limited to three integral parameters of the mean flow available from all computations: the momentum thickness θ , the shape factor H , and the friction factor C_f . Mean profile comparisons were made by many authors and a few even made comparison with turbulence data.

Fig. 1 shows the common comparison for the easiest flow, a flat plate boundary layer. On shifted scales we show H , C_f (CF) and R_θ (RTH) vs. x for the 29 methods examined at the conference. The letters on the left identify the method. Note that all but one method is able to handle this flow reasonably adequately (see TBLPC-1 for method code key).

Fig. 2 shows the comparisons for a more difficult flow, an "adverse" pressure gradient (decelerating free-stream) flow. Note that some methods do reasonably well while others do quite poorly. One predictor exemplified the integrity of the conference by producing a calculation that failed to fit his own data!

A small committee headed by H. Emmons studied the results and attempted to rank the methods. Fig. 3 shows a comparison of the rankings of two evaluation committee members. Methods based on partial differential equations are shown as P , those including a turbulence differential equation are indicated by P^+ , and integral methods are shown as I . The committee noted that several different kinds of methods performed quite well, and that certain methods were consistently poor. They went on to recommend abandoning the poor methods in view of the success of the better ones.

While there were a number of successful and attractive integral methods tested at the conference, one had to be impressed

with the generality and speed of computations based on the partial differential equations. These schemes can be extended to new situations much more readily than integral methods. While integral methods are indeed useful in certain special cases, there is a definite interest in use of partial differential equation schemes. In view of the advantages of partial differential equation methods, we have omitted integral methods from further consideration in this review. However, the development of adequate partial differential equations may well stimulate development of new integral methods based upon these equations. Two of the better TBLPC integral methods were developed in this spirit (Mc Donald and Camarata, Hirst and Reynolds in TBLPC-1).

3. Status of Closure Experiments

In time averaging the Navier-Stokes equations to render the turbulent flow problem tractable, information is lost to the point that the resulting equations are not closed. Additional equations may be derived by manipulations with the Navier-Stokes equations before the averaging process, but the number of independent unknowns increases more rapidly than the number of equations, and rigorous closure is just impossible. Apart from direct numerical solution of the unaveraged equations, about which we will comment later, the only hope lies in replacing some of the unknowns in the equations by terms involving other unknowns to bring the number of unknowns down to the number of describing equations. Such assumed relations are called "closure assumptions".

In turbulent shear flows it has seemed most convenient to work with the velocities as independent field variables (rather than with their fourier transforms as is often done in isotropic turbulence). The simplest closure involves only the mean momentum equations, which contain unknown turbulent stresses for which a closure assumption must be made. This is the MVF closure (Mean Velocity Field). Models of this sort have been applied to a wide variety of flows, and work quite well for most boundary layer flows of the Stanford conference. MVF methods are denoted by P in Fig. 3.

The next formal level of closure is at the level of the dynamical equations for the turbulent stresses, which we shall call mean Reynolds stress closures (MRS). There have only been a few experimental calculations at this level, and such closures are not yet tools for practical analysis.

An intermediate closure level using the dynamical equation for the mean turbulent kinetic energy (MTE closure) has dominated more recent calculations, and has developed to the point of utility as an engineering tool. MTE closures are denoted by P^+ in Fig. 3. Since MTE closures permit calculation of at least one feature of the turbulence, such methods work better than MVF closures in problems where the turbulence behavior lags behind sudden changes in conditions. In addition, they give more useful information for only a little additional effort, indeed for considerably less effort than MRS closures. They do not give adequate detail on the turbulent structure and do not work well when the structure (but not the energy) depends explicitly upon some effect, such as rotation. MRS closures will be needed for these problems (although MRS closures have not yet been tested in cases where they are really needed to obtain accurate mean velocity predictions). It would appear, then, that MTE closures will remain important for some time, serving both as useful engineering tools and as guides to the development of more complex models.

Another approach that has promise for study of turbulence structure is the fluctuating velocity field (FVF) closure used by Deardorff (1970). Using the analog of a MVF closure for turbulent motions having scales smaller than his computational mesh, Deardorff carried out a three-dimensional unsteady solution of Navier-Stokes equations, thereby calculating the structure of the larger scale eddy motions. It is likely that such calculations will remain beyond the reach of most for some time to come, and that we will have to content ourselves with whatever we can extract from the computationally much simpler MVF, MTE, and MRS closures. However, results like Deardorff's should serve as guides for framing closure models.

Truly fresh approaches to turbulence have not been frequent, and this review would not be complete without the mention of two that show promise for future research. The first is Busse's (1970) and Howard's (1963) work in fixing bounds on the overall transport behavior of turbulent flows without any closure approximations. The second is the use of multipoint velocity probability densities (Lundgren 1967, Fox unpublished) with closure assumptions being made on the probability densities rather than on velocity moments. Neither of these schemes is presently developed as general analytical tool, but either could spark a major revolution in turbulence theory.

In the sections that follow we will outline the theoretical framework of the MVF, MTE, and MRS closures, and present examples and commentary on applications of each method. Readers unfamiliar with the differential equations should consult Hinze (1959) or Townsend (1956). In several instances I have taken the liberty to reformulate the constitutive models in an effort to extend their generality.

Following up on the concerns expressed about invariance at TBLPC, I have made extensions that put the basic equations in a properly invariant manner. One must not read too much into this, however. Bradshaw (1970) cites Russell's (1961) wisdom: "A philosophy which is not self-consistent cannot be wholly true, but a philosophy which is self-consistent can very well be wholly false ... There is no reason to suspect that a self-consistent system contains more truth."

4. MVF Closure Theory

The equations for the mean velocity field U_i and pressure P in an incompressible fluid with constant density and viscosity are

$$\frac{\partial U_i}{\partial x_i} = 0 \tag{4.1a}$$

$$\frac{\partial U_i}{\partial t} + U_j \frac{\partial U_i}{\partial x_j} = - \frac{1}{\rho} \frac{\partial P}{\partial x_i} + \nu \frac{\partial^2 U_i}{\partial x_j \partial x_j} - \frac{\partial R_{ij}}{\partial x_j} \tag{4.1b}$$

where $R_{ij} = \overline{u_i u_j}$. We will loosely call R_{ij} the Reynolds stress tensor (actually $-\rho R_{ij}$ is the stress tensor). The over bar denotes a suitable average, and u_i is the instantaneous fluctuation field.

One obtains closure through assumptions that relate the Reynolds stresses R_{ij} to properties of the mean velocity field U_i . The most productive approach has been to use a consitutive equation involving a turbulence length scale, usually called the "mixing length". A generalization of the usual assumption is

$$R_{ij} = \frac{q^2}{3} \delta_{ij} - 2\sqrt{2S_{mn}S_{mn}}\ \ell^2\ S_{ij} \tag{4.2a}$$

where $S_{ij} = \frac{1}{2}(\frac{\partial U_i}{\partial x_j} + \frac{\partial U_j}{\partial x_i})$ (4.2b)

is the strain-rate tensor, $q^2 = R_{ii} = \overline{u_i u_i}$, and ℓ is a turbulence length scale. Throughout we shall denote such length scales by ℓ , often subscripted. For the special case of simple shearing motion, where

$$S_{ij} = \begin{pmatrix} 0 & \frac{1}{2}\frac{dU}{dy} & 0 \\ \frac{1}{2}\frac{dU}{dy} & 0 & 0 \\ 0 & 0 & 0 \end{pmatrix} \tag{4.3}$$

(4.2) gives

$$R_{ij} = \begin{pmatrix} q^2/3 & -\ell^2 \left|\frac{dU}{dy}\right| \frac{dU}{dy} & 0 \\ -\ell^2 \left|\frac{dU}{dy}\right| \frac{dU}{dy} & q^2/3 & 0 \\ 0 & 0 & q^2/3 \end{pmatrix} \tag{4.4}$$

Now, if the spatial distribution of ℓ is assumed, (4.1) and (4.2) form a closed system of equations for the variables U_i and $P + \rho q^2/3$. Note that the combination of $\rho q^2/3$ with P means that q^2 need not be evaluated.

Another closure approach used at this level is generalized as

$$R_{ij} = \frac{q^2}{3}\delta_{ij} - 2\,\nu_T S_{ij} \tag{4.5}$$

where ν_T is the turbulent or eddy (kinematic) viscosity. An assumption of the spatial distribution of ν_T also suffices for closure. Occasionally these approaches are mixed. Comparison of (4.2) and (4.5) gives

$$\nu_T = \ell^2 \sqrt{2 S_{mn} S_{mn}} \tag{4.6}$$

and consequently assumptions about ℓ are often used to determine ν_T, or vice versa.

Mellor and Herring (1970b, hereafter referred to as MH), observing that (4.2) or (4.5) imply that the Reynolds stresses deviations from $q^2/3\ \delta_{ij}$ are proportional to the strain rates (and hence that the principal axes of the stress deviation and strain-rate are aligned), call these closures "Newtonian". Accordingly, we denote them by MVFN. The success of the Newtonian model is remarkable, especially since for even the weakest of turbulent shear flows the principal axes are not aligned (Champagne, Harris, and Corrsin 1970).

In MVFN calculations the mixing length ℓ is assumed in terms of the geometry of the flow. In a thin free shear layer, such as a jet or wake, the assumption that ℓ is proportional to the local width of the layer seems to work quite well, with something like

$$\ell = 0.16 \tag{4.7}$$

This behavior is also used in the outer region of a turbulent boundary layer. Near a wall ℓ is experimentally found to be proportional to the distance from the wall, and

$$\ell = \kappa y \qquad \kappa \lesssim 0.41 \tag{4.8}$$

seems to hold for smooth walls, rough walls, with modest compressibility, with transpiration, and in just about any axial pressure field.

In the viscous region immediately adjacent to a wall the calculations are improved if ℓ is reduced, with

$$\ell = \kappa y[1-\exp(-\frac{yu^*/\nu}{A^+})] \qquad (4.9)$$

where $u^* = \sqrt{\tau_w/\rho}$ is the friction velocity based on the local wall shearing stress τ_w, and A^+ is a parameter characterizing the thickness of the viscous region on the familiar $y^+=yu^*/\nu$ scale. A^+ is known to depend upon both the streamwise pressure gradient and the transpiration velocity (for suction or blowing). Physical models of the wall layer can be used to suggest (4.9).

Kays and his associates (private communication) have correlated their turbulent boundary layer data to produce the A^+ correlation shown in Fig. 4 . There P_o^+ is the streamwise pressure gradient parameter

$$P_o^+ = \frac{\nu}{\rho u^{*3}} \frac{dP}{dx} \qquad (4.10a)$$

and V_o^+ is the transpiration parameter

$$V_o^+ = V_o/u^* \qquad (4.10b)$$

where V_o is the injection velocity normal to the porous wall. Kays also modifies (4.9) by using the <u>local</u> shear stress $\tau(y)$ rather than τ_w in u^* .

In boundary layer calculations, most workers simply use zonal models, with (4.9) in the inner region (which becomes (4.8) further from the wall) and something like (4.7) in the outer portion of the flow. Byrne and Hatton (1970) use a three-layer model as the basis for ν_T assumptions. MH have used concepts from the theory of matched asymptotic expansions to obtain composite representation for ℓ valid across an entire turbulent boundary layer. A typical distribution of ℓ in a boundary layer is shown in Fig. 5.

For steady, two-dimensional incompressible boundary layers the MVFN equations reduce to $(U_i = (U,V,W),\ x_i = (x,y,z))$

$$\frac{\partial U}{\partial x} + \frac{\partial V}{\partial y} = 0 \tag{4.11a}$$

$$U \frac{\partial U}{\partial x} + V \frac{\partial U}{\partial y} = - \frac{1}{\rho} \frac{\partial P_\infty}{\partial x} + \frac{\partial}{\partial y} (-\overline{uv}) \tag{4.11b}$$

and

$$-\overline{uv} = \ell^2 \left|\frac{dU}{dy}\right| \frac{\partial U}{\partial y} \tag{4.11c}$$

or

$$-\overline{uv} = \nu_T \frac{dU}{dy} \tag{4.11d}$$

These equations are of parabolic type, and may be solved by a forward marching technique. The upstream profile $U(x_o,y)$ must be specified, and the free-stream pressure distribution $P_\infty(x)$ must be known. $V(x_o,y)$ is then determined by (4.11a). The numerical problems are straightforward but not a trivial aspect of a successful method. Implicit schemes have been most successful, although explicit marching methods can be used if the wall region is treated separately.

In order to handle the rapid variations near a wall, one must either use a fine computational mesh in this region or else employ a special treatment. The variation in shear stress is, to a first approximation, small across this region, and the "law of the wall" is known to be followed by the mean velocity profile very near the wall for most turbulent boundary layers. One simple approach is therefore to patch the numerical solution at the first computation point away from the wall to the empirical wall law,

$$\frac{U}{u*} = \frac{1}{\kappa} \ell n \left(\frac{yu*}{\nu}\right) + B \qquad \frac{yu*}{\nu} > 30 \tag{4.12}$$

$$B \simeq 5$$

This sets the value of U in terms of the wall shear stress (taken as the shear stress at the first mesh point) and y value at that point, and V may be taken as zero (or V_o) there. These conditions then provide boundary conditions for the numerical solution in the outer part of the flow, and a nearly uniform computational mesh in the outer region is usually feasible.

For transpired boundary layers or strong favorable pressure gradients the shear stress variation in the wall region is significant and a better analysis is required. One approach is to use a solution to the governing equations obtained by assuming parallel flow (neglecting axial derivatives, except for pressure). This "Couette flow" solution is obtained by analytical or numerical solution of ordinary differential equations, and these solutions may often be precomputed in parametric form. A semi-theoretical wall layer treatment of this sort is very effective in permitting large computational steps in the streamwise direction.

The Couette flow analysis uses the constitutive equation as its basis. The total shear stress in the boundary layer is written as

$$\frac{\tau}{\rho} = (\nu + \nu_T) \frac{\partial U}{\partial y} \tag{4.13}$$

Eq. (4.13) may be integrated and expressed in dimensionless form,

$$\frac{U}{u*} = \int_0^{y^+} \frac{\tau^+}{(1+\nu_T/\nu)} \, dy^+ \tag{4.14}$$

where $y^+ = yu*/\nu$ and $\tau^+ = \tau/\tau_w$. Thus, to develop the inner region solutions one needs to know the shear stress distribution $\tau(y)$. In the Couette flow approximation the convective terms are deleted, and the shear stress emerges from the momentum equation as

$$\tau^+ = 1 + U^+V_o^+ + P^+y^+ \tag{4.15}$$

Loyd, Moffat, and Kays (1970) have found this inadequate for strongly accelerated flows beyond $y^+ = 5$. Since the patching will take place at a much larger value of y^+ (perhaps around 30-50), a better shear stress distribution is needed. Loyd et al noted that for fully asymptotic flow, where $U/U_\infty = f(y/\delta)$ throughout the entire layer (such flows can be realized with strong acceleration), the shear stress distribution is

$$\tau^+ = 1 + U^+V_o^+ + P^+y^+ \left[1 - \frac{1}{y}\int_o^y \left(\frac{U}{U_\infty}\right)^2 dy\right] \qquad (4.16)$$

and they use this expression to obtain a better shear stress distribution for use in the Couette analysis. These integrations are carried out at each streamwise step in the computation to patch the inner and outer solutions.

Recently Kays has found that improvements in the prediction of flows with sudden changes in wall conditions are possible if empirical "lag equations" are used for the parameters P^+ and V_o^+ used to determine A^+ from the correlation of Fig. 4. Loyd, Moffat, and Kays (1970) use

$$\frac{dP_e^+}{dx^+} = \frac{P^+ - P_e^+}{C_1} \qquad \frac{dV_{oe}^+}{dx^+} = \frac{V_o^+ - V_e^+}{C_2} \qquad (4.17a,b)$$

with C_1 and C_2 of approximately 3000. Here P^+ and V_o^+ are the actual values, and P_e^+ and V_{oe}^+ are the "effective" values used in reading A^+ from Fig. 4, and $x^+ = xu_*/\nu$.

Fine wall mesh schemes have been used to avoid this patching process. It is critical to use a good implicit difference scheme in this case. Mellor (1967) developed a good linearized iteration technique which has since been adopted by others.

The approach to calculation of the temperature field and heat transfer follows closely the hydrodynamic calculation outlined above. For incompressible flow of a fluid with constant and uniform properties, neglecting the input to the thermal field by viscous dissipation, the thermal energy equation (obtained by a combination of the energy and momentum equations) is

$$\frac{\partial \Theta}{\partial t} + U_j \frac{\partial \Theta}{\partial x_j} = \alpha \frac{\partial^2 \Theta}{\partial x_j \partial x_j} - \frac{\partial}{\partial x_j} (\overline{u_j \theta}) \qquad (4.18)$$

Here Θ denotes the mean temperature and θ the local temperature fluctuation. The terms $\overline{u_j \theta}$ represent transports of internal energy by turbulent motions, and it is these terms that bring the closure problem.

The common approach to the thermal problem is to assume

$$-\overline{u_j \theta} = \alpha_T \frac{\partial \Theta}{\partial x_j} \qquad (4.19)$$

where α_T is the "turbulent diffusivity for heat", analogus to ν_T. With knowledge of α_T, and with U_j from solution of the hydrodynamic problem, the thermal problem is closed. It is usually assumed that

$$\nu_T / \alpha_T = Pr_T \qquad (4.20)$$

where Pr_T is a turbulent Prandtl number. For gases Pr_T is experimentally found to be approximately 0.7-1 in typical boundary layer flows, and a constant value often suffices. More elaborate correlations of Pr_T with other properties of the flow have also been proposed (Simpson, Whitten, and Moffat 1970, Cebeci 1970b). The choice of Pr_T is particularly important for liquid metal heat transfer.

In examining the nature of α_T and ν_T in the viscous region of boundary layers, use has often been made of an unsteady two-dimensional parallel flow Stokes model (Cebeci 1970b). While such analysis may well yield the relevant dimensionless groupings, and possibly a fairly reasonable form for the α_T and ν_T distributions, failure to consider the now well established strong three-dimensional unsteady features of the laminar sublayer (Kline, et al 1967) would seem to render quantitative results questionable. Since the heat transfer rate in boundary layers is strongly dependent on the assumptions made in this region, it would seem that at present the best results will be obtained with models having high empirical content, such as the A^+ correlation of Fig. 4 and the Pr_T correlations of Simpson et al (1970). New theories based on more accurate models of the wall layer will probably get considerable attention.

Though the concept of a turbulent viscosity has been displeasing to many, one cannot deny the success that its users have enjoyed. An interesting interpretation of ν_T is obtained by multiplying (4.5) by S_{ij}, viz.

$$\frac{\nu_T}{\nu} = \frac{-R_{ij}S_{ij}}{2\nu S_{mn}S_{mn}} \tag{4.21}$$

The numerator is the rate of production of turbulence energy, and the denomenator is the rate of dissipation of mechanical energy by the mean field.

5. MVF Calculation Examples

Many examples of MVF calculations have now been published, and we shall now look at a small but representative collection. Readers should see the original papers for description of the details.

Most published computations have dealt with boundary layers. The numerical techniques employed have varied considerably, and hence computational costs initially varied widely between programs. But now most workers have adopted implicit difference schemes, with special wall region treatment as outlined above, and/or a linearized iteration technique (Mellor 1967), so that run times are now reasonably uniform. A typical two-dimensional compressible boundary layer can now be treated in under one minute on a typical large computer.

Among the pioneers and current advocates of the MVFN equations were A. M. O. Smith, and his colleagues, chiefly T. Cebeci. They elect to specify the eddy viscosity distribution, using a form derived from the mixing length model in the inner region and a uniform value reduced by multiplication by an intermittency factor in the outer region. The curves marked CS on Figs. 1 and 2 are by their method. Cebeci et. al. (1969, 1970a) have extended their method to include heat transfer and compressibility.

D. B. Spalding has been an active explorer of turbulent boundary layer computational methods. His early work with Patankar (1967) was based on the MVFN equations with mixing length specifications, and their complete program descriptions served as the seed for numerous computational efforts elsewhere. Fig. 6 shows their computation of a wall jet flow as presented in TBLPC-1. This computation was among the few "more difficult" flows voluntarily presented by predictors to illustrate the range of their

method. Spalding has now essentially abandoned this method in favor of MTE models.

G. Mellor and his coworkers have used MVF closures for a variety of problems, and their unpublished work on the theoretical foundations of the theory has been both educational and useful in writing this review. Mellor and Herring startled TBLPC by presenting two methods, one based on MVF closure and a second based on MTE closure; except in one case the H, θ, and C_f predictions by the two methods were absolutely indistinguishable, both being judged among the best at the conference (shown as MH on Figs. 1 and 2). Mellor (1967) has also used a MVF method to study certain classes of three-dimensional boundary layers, and Herring and Mellor (1968) have extended the method to compressible boundary layers.

Since TBLPC, interest in the MVFN prediction methods has spread. F. Dvorak (private communication) has been looking at applications to more difficult flows of interest in aircraft design, and has kindly provided Fig. 7 as an illustration of his work. With some adjustment of the eddy viscosity prescription, Dvorak is able to predict the growth of a boundary layer with tangential injection upstream and a strong adverse pressure gradient. This flow has two overlaid mixing layers, which suggests the variation in ν_T used by Dvorak, though it would seem difficult to make really accurate calculations if the downstream data were not available to guide the ν_T tailoring.

The MVFN equations have been used in the calculation of three-dimensional boundary layer flows by Mellor (1967) and currently by Wheeler and Johnston (unpublished). We remark that the MVFN model assumes that the shear stress is aligned with the strain rate. In spite of the strong experimental evidence (Johnston 1970) that this does not hold, the MVFN equations work

remarkably well in predicting the mean velocity field in three-dimensional boundary layer flows where the pressure field (rather than the turbulent stress field) has the primary influence on the three-dimensionality (most boundary layers of engineering interest may be of this type). Fig. 8 includes integral parameter predictions using Mellor and Herring's MVFN method by Wheeler and Johnston (private communication) of the flow along the symmetry plane in a boundary layer approaching an obstacle. Except very near the separation point, results are excellent. The MTE predictions on Fig. 8 will be discussed in Section 7.

The prediction of turbulent boundary layer separation by MVF methods has not been very successful. Indeed, it may be appropriate to identify turbulent separation in terms of the turbulence near the wall, and this will require use of a more sophisticated model (MTE or MRS), quite possibly in their full (rather than boundary layer) form.

MVFN methods have been used with some success in compressible flows. Fig. 9 shows a prediction of Herring and Mellor (1968) of the Mach number correction to the skin friction factor for a flat plate boundary layer. Fig. 10 shows their prediction for the boundary layer on a waisted body of revolution. Note that, while the momentum thickness is quite accurately predicted, the velocity profile details are in considerable error. Indeed, MVFN methods are often much better in predicting integral properties of the flow than in predicting local details. Geometrical effects neglected in the analysis are the probable cause of much of the discrepancy.

Fig. 11 shows a prediction by Healzer and Kays (private communication) of the heat transfer coefficient (based on enthalpy difference) in an adiabatic rocket nozzle boundary layer flow, made with an extended MVFN method (no chemical reactions

considered). The accuracy of this prediction attests to the value of such methods in contemporary engineering analysis.

MVFN methods have been used in contained and recirculating flows, where the boundary layer approximations no longer apply. Spalding and his coworkers have led these efforts (see Gosman, et al 1969). The numerical treatment is critical here, for the equation system is elliptic rather than parabolic, and the entire field must be solved simultaneously. Computational times are consequently considerably longer, with several minutes being required for a typical flow. Recently Chin and Seban (private communication) studied an improvement of Spalding's upwind difference treatment as applied to the flow in a cavity under a turbulent shear flow. The results of their computation are shown in Fig. 12. They used a simple wall region patching treatment, with a linear mixing length near the walls, a uniform mixing length in the central region of the cavity, and a constant mixing length in the external shear layer. The computational mesh was 41 x 41 in the cavity, with closer spacing near the walls. In order to obtain convergence in the solution of the difference equations, over 1000 relaxation iterations were required, and the computation took 20 minutes on a CDC 6400 computer. While the velocity distribution in the central cavity is predicted very well, the heat transfer from the cavity bottom is not. Seban (private communication) states that an improved wall region treatment is required, but that the relaxation iteration became nonconvergent when this was tried. He suggested that perhaps the time-dependent MVFN equations would have to be solved in order to compute the final steady-state flow.

MVFN equations have not been tested in very many time-dependent flows, for there is practically no comparison data. Moreover, the computation costs skyrocket with every added dimension. However, if the time-dependence is periodic, a fourier analysis can be used to reduce the problem to a sequence of steady

problems. If the flow is parallel and the periodic component takes the form of streamwise travelling waves of small amplitude, then the MVFN equations may be reduced to ordinary differential equations for the periodic disturbance similar in structure to those used in analysis of the stability of laminar flows. We have been looking at the results of such computations for periodic disturbances in shear flows and for flows over waving boundaries. Our experimental observations of small periodic disturbances in turbulent channel flow (Hussain and Reynolds 1970) indicate that a dispersion relation exists between the frequency and streamwise wavenumber of disturbance eigenfunctions. Fig. 13 shows our predictions for this relationship as compared with our experimental data. The predictions were made using the eddy viscosity distribution calculated from the mean velocity profile, a fine wall mesh, and (4.5) in the time-dependent MVFN equations. Note that the MVFN model seems to work well in this unsteady flow.

We have also applied this approach to flows over waving boundaries, and in particular to Kendall's (1970) flow and Stewart's (1970) flow. In neither case did our predictions agree with the measurements; Davis (1970) used a similar MVF model with curvilinear coordinates, apparently with greater success. An experiment on turbulent channel flow with a waving wall has just been completed in our laboratory. The wave-induced wall pressure oscillation is predicted fairly well by MVF theory for upstream-running waves, but not at all well for downstream-running waves. This suggests that the MVF model is weakest in flows with a "critical layer", i.e. a point where the mean velocity matches the wave speed. The ability to predict such flows by MVF methods would seem questionable, in view of the rapid changes in strain rate to which the turbulence is subjected, and in all probability a MTE or MRS method would work much better. We intend to explore calculations along these lines.

MVF methods fail in any flow where the nature of the turbulence is altered by some parametric effect, such as rotation, which does not appear parametrically in the equations of mean motion. Such effects can be included in MVF methods only by alteration of the ℓ or ν_T specification, and hence MTE or MRS methods are clearly to be preferred for such cases.

The most ambitious application of MVFN equations has been to atmospheric general circulations. The National Center for Atmospheric Research (NCAR) has developed an elaborate model in which the velocity components, temperature, and humidity are calculated over the entire earth. The goal is to obtain an accurate 14-30 day weather forecast. The computational mesh involves six vertical layers and 5° grid spacing at the equator, with fewer points near the poles. The horizontal grid therefore varies from about 500 km to 100 km on a side. A turbulent viscosity model is used to handle sub-grid scale turbulence. The effects of sun, show, water, mountains, and precipitation are simulated. The main features of global weather patterns are reproduced. The dearth of field data make quantitative comparison difficult, and initialization almost impossible. Kasahara (1969) reports that "better" results are obtained with a 2.5° mesh, but with present computers a 24-hour computation requires about 24 hours with this finer mesh. Fig. 14 shows an NCAR computation from the 5° model. It seems quite possible that such calculations will someday become a routine part of our weekly weather forecasts, though refinements in the physical model may be required.

6. MTE Closure Theory

The MVF equations assume that the turbulence adjusts immediately to changes in mean conditions, and that a universal relationship exists between the turbulent stresses and the mean strain rates. To avoid these assumptions one must include differential equations for the Reynolds stresses (called "dynamical" or "transport" equations). MRS closures use these equations; MTE closures are somewhat simpler, and employ a single equation for the turbulent kinetic energy in conjunction with some constitutive or structural equations relating the turbulent stresses to the turbulent kinetic energy. Thus, MTE methods can to a degree handle the delayed response of turbulence structure to sudden changes in mean conditions, and are now being studied by several groups for use in such problems.

Equations for the R_{ij} may be developed from the Navier-Stokes equations (Townsend 1956; Hinze 1959). These are

$$\frac{\partial R_{ij}}{\partial t} + U_k \frac{\partial R_{ij}}{\partial x_k} = - R_{ik} \frac{\partial U_j}{\partial x_k} - R_{jk} \frac{\partial U_i}{\partial x_k}$$

$$- \frac{\partial}{\partial x_k} (\overline{u_i u_j u_k}) - \frac{1}{\rho} [\frac{\partial}{\partial x_j} (\overline{u_i p}) + \frac{\partial}{\partial x_i} (\overline{u_j p})]$$

$$+ \overline{\frac{p}{\rho} (\frac{\partial u_i}{\partial x_j} + \frac{\partial u_j}{\partial x_i})} + V_{ij} \qquad (6.1)$$

Here V_{ij} is the viscous term to be discussed shortly. A contraction of these equations gives the equation for the turbulent kinetic energy. With $q^2 = \overline{u_i u_i}$, this may be written as

$$\frac{\partial q^2/2}{\partial t} + U_k \frac{\partial q^2/2}{\partial x_k} = - R_{ik} \frac{\partial U_i}{\partial x_k} - \frac{\partial}{\partial x_k} (\overline{u_k u_i u_i}/2)$$

$$- \frac{1}{\rho} \frac{\partial}{\partial x_k} (\overline{u_k p}) + V_{ii}/2 \qquad (6.2)$$

The first term on the right is the "turbulence production". The more common form of V_{ij} is

$$V_{ij} = \nu \frac{\partial^2 R_{ij}}{\partial x_k \partial x_k} - 2\mathscr{D}_{ij} \qquad (6.3a)$$

where

$$\mathscr{D}_{ij} = \nu \overline{\frac{\partial u_i}{\partial x_k} \frac{\partial u_j}{\partial x_k}} \qquad (6.3b)$$

Then,

$$\frac{V_{ii}}{2} = \nu \frac{\partial^2 q^2/2}{\partial x_k \partial x_k} - \mathscr{D} \qquad (6.3c)$$

where

$$\mathscr{D} = \mathscr{D}_{ii} \qquad (6.3d)$$

This form is appealing because the first term in $V_{ii}/2$ can be interpreted as a "gradient diffusion" of turbulent kinetic energy, and the second is negative-definite (suggestive of "dissipation" of turbulence energy). However, the rate of entropy production is proportional to

$$\epsilon = \nu \overline{(\frac{\partial u_i}{\partial x_j} + \frac{\partial u_j}{\partial x_i}) \frac{\partial u_i}{\partial x_j}} \geq 0 \qquad (6.4)$$

Properly ϵ is called the "dissipation", but not $\mathscr{D}$. We might call $\mathscr{D}$ the "isotropic dissipation".

A second form of V_{ij} is

$$V_{ij} = \nu \frac{\partial}{\partial x_k} \overline{[u_i \sigma_{jk} + u_j \sigma_{ik}]}$$

$$- \nu \overline{[\sigma_{jk} \frac{\partial u_i}{\partial x_k} + \sigma_{ik} \frac{\partial u_j}{\partial x_k}]} \qquad (6.5a)$$

where

$$\sigma_{ij} = \frac{\partial u_i}{\partial x_j} + \frac{\partial u_j}{\partial x_i} \qquad (6.5b)$$

For which (6.5a),

$$\frac{V_{ii}}{2} = \nu \frac{\partial}{\partial x_k} \overline{[u_i \sigma_{ik}]} - \epsilon \qquad (6.5c)$$

The appearance of ϵ makes this form appealing, even though the first term can no longer be interpreted as "gradient diffusion".

MTE methods require closure assumptions for the last three terms in (6.2) and there has been heated debate on this point. There seems to be universal agreement that the dissipation term should be modeled by the constitutive equation

$$\epsilon = C \frac{q^3}{\ell_\epsilon} \qquad (6.6)$$

where ℓ_ϵ is a "dissipation length scale", and C is a function of the dissipation Reynolds number $R_\epsilon = q\ell_\epsilon/\nu$, C being constant for $R_\epsilon \gg 1$. Note that for $R_\epsilon \gg 1$ ϵ is independent of ν; this is a reflection of the belief that the small scale eddies responsible for the final dissipation of mechanical energy can handle all the energy that is fed to them from and by larger scale motions, and hence the larger eddies control the dissipation rate. The spectral transfer process for $R_\epsilon > 1$ results from the

inertial non-linearity, which suggests (6.6). The remainder of the viscous term is only important very near a wall; though it is strictly incorrect, reasonable results have been obtained by taking $\mathcal{D} = \epsilon$, and writing

$$V_{ii}/2 = \nu \frac{\partial^2 q^2/2}{\partial x_j \partial x_j} - \epsilon \qquad (6.7)$$

MH's model is more complicated (see 8.10, 6.22).

The main MTE argument stems over the treatment of the pressure-velocity correlation term and the triple velocity correlation term. One widely used approach is the "gradient diffusion" model, where one sets

$$\overline{(u_k \frac{p}{\rho} + u_k \frac{u_i u_i}{2})} = -N_Q \nu_T \frac{\partial q^2/2}{\partial x_k} \qquad (6.8)$$

where N_Q is a constant (or specified function). There is strong feeling in some quarters that this model ignores the dominance of transport processes by large scale eddy motions. A generalization of a "large eddy transport" model (Bradshaw, Ferriss, and Atwell 1967) is

$$\overline{(u_k \frac{p}{\rho} + u_k \frac{u_i u_i}{2})} = G q^2 Q_k \qquad (6.9)$$

where G is a constant (or specified function) and Q_k is a global vector velocity scale characteristic of the large eddy motions. The choice for this closure is of considerable importance; neglecting the viscous diffusion terms, the equation system based on (6.8) is of elliptic type, while with (6.9) the system is hyperbolic. This mathematical difference is suggestive of substantial physical differences in the model. Both approaches have been used quite successfully, however, and it is not easy to make a strong case for either solely by testing against experiments.

Having closed the q^2 equations, one must relate the Reynolds stresses to q^2 in order to have a closed system. Again two approaches have been hotly debated. The more common approach uses the constitutive equation (4.5), together with an additional constitutive equation relating the turbulent viscosity to the turbulent kinetic energy,

$$\nu_T = q\ell F(R_T) \tag{6.10}$$

Here ℓ is a turbulence length scale, and F describes the dependence upon the turbulence Reynolds number $R_T = q\ell/\nu$ with $F = \text{const.}$ for $R_T \gg 1$. The length scales ℓ and ℓ_ϵ must be specified (either algebraically or through a differential equation) to close the equation system. Since use of (6.10) again implies Newtonian behavior, we shall refer to this MTE closure as MTEN.

Observing that the Newtonian structure is never observed in turbulent shear flows, but that persistently strained flows apparently develop an "equilibrium structure", Bradshaw prefers to relate the Reynolds stresses directly to q^2. A generalization of his constitutive equation is

$$R_{ij} = a_{ij}q^2 \tag{6.11}$$

where a_{ij} depends upon the type of strain. For the case of pure shear (4.3), a reasonable form of (6.11) is (see Townsend 1956, Champagne, Harris and Corrsin 1970)

$$a_{ij} = \begin{pmatrix} 0.48 & -0.16 & 0 \\ -0.16 & 0.26 & 0 \\ 0 & 0 & 0.26 \end{pmatrix} \tag{6.12}$$

Lighthill (1952) suggested a general form which gives $a_{12} = -0.16$ but does not correctly represent the diagonal terms,

$$a_{ij} = \frac{1}{3}\delta_{ij} - \frac{0.32\ S_{ij}}{\sqrt{2S_{mn}S_{mn}}} \qquad (6.13)$$

We will denote MTE closures involving an assumed turbulence structure (e.g. 6.12) by MTES

One would like to assume constant values for a_{ij} in thin shear layers. However, on a symmetry axis i a pipe or free jet flow, where $R_{12} = 0$, $a_{12} = 0$, and hence to use (6.11) in such flows one must specify a variation in a_{ij}. Hence, one must have a good "feel" for the flow to obtain a good prediction. This requirement for intuition is less important in simpler boundary layer flows, where a uniform value of a_{ij} produces reasonable results.

There is a more fundamental objection to the MTES idea. Recently Lumley (1970) has argued that the homogeneous flows upon which (6.11) and (6.12) are based do not really reach equilibrium, and that instead the turbulence time (and length) scales continually increase. Champagne, Harris, and Corrsin's(1970) experiments confirm this expectation. Hence, a structural model cannot be fully correct in homogeneous flows.

MTEN and MTES closures both fail in the case of a sudden removal of the mean strain rate, where it is known that a very slow relaxation of the structure towards isotropy takes place. The MTEN model instantly becomes isotropic, which the MTES model retains a permanent structure (unless one twiddles with the a_{ij}). This may not be a serious objection as long as these methods are used in shear flows having reasonably persistent strain.

To summarize, the MTE closures commonly employed use one of the following two forms: Using (4.5), (6.6), (6.7), (6.8), and (6.10), with $\ell = \ell_\epsilon$,

$$\frac{\partial q^2/2}{\partial t} + U_j \frac{\partial q^2/2}{\partial x_j} = 2\nu_T S_{ij}S_{ij} - C \frac{q^3}{\ell}$$

$$+ \frac{\partial}{\partial x_j}\left[(N_Q \nu_T + \nu \frac{\partial q^2/2}{\partial x_j}\right] \qquad (6.14a)$$

$$\nu_T = q\ell F \qquad (6.14b)$$

Or, using (6.6), (6.7), (6.9), and (6.11)

$$\frac{\partial q^2/2}{\partial t} + U_j \frac{\partial q^2/2}{\partial x_j} = - a_{ij}q^2 S_{ij} - C \frac{q^3}{\ell}$$

$$- \frac{\partial}{\partial x_k}(Gq^2 Q_k) + \nu \frac{\partial q^2/2}{\partial x_j \partial x_j} \qquad (6.15)$$

For (6.14) values or distributions for C , F , and N_Q must be assumed, while for (6.15) values or distributions for a_{ij} , C , G , and Q_k are needed. Both forms require an assumption for the spatial distribution of the length scale ℓ . The terms with ν are not important except very near walls, and are often neglected in the outer flow.

Most computations have used length scale distributions of the sort described in Section 4 above. Recently there has been some interest in using a differential equation for ℓ , and the most extensive test of this approach has been by Rodi and Spalding (1970), and Ng and Spalding (1970). Their length scale equation, which is based on a spectral transport equation (Rotta 1951), can be generalized with slight modification as

$$\left(\frac{\partial}{\partial t} + U_j \frac{\partial}{\partial x_j}\right)\left(\frac{\ell q^2}{2}\right) =$$

$$C_1 \nu_T \ell S_{ij} S_{ij} - C_2 q^3 + C_4 \frac{\partial}{\partial x_j}\left[\nu_T \frac{\partial}{\partial x_j}(\ell q^2/2)\right] \tag{6.16}$$

Spalding and his coworkers are able to obtain very good predictions of a variety of boundary layer and free shear flows using (essentially) (6.16) to determine ℓ, provided some adjustments in C_2 are made near solid walls.

Gawain and Pritchard (1970) proposed a more complicated hueristic integro-differential equation for turbulent length scales. In effect their local length scale is determined by the mean velocity field in the region of the local point. The two-point tensor

$$\mathcal{R}_{ij}(x, \xi) = \frac{\overline{u_j(x + \xi)u_j(x - \xi)}}{\overline{u_k u_k}} \tag{6.17}$$

is used to define the length scale,

$$\ell^2 = \int \mathcal{R}_{ii}\, \xi^2 dV / \int \mathcal{R}_{ii} dV \tag{6.18}$$

where dV denotes a volume integration. A form for $\mathcal{R}_{ii}$ is in effect assumed in terms of the mean velocity field, and the integrations are performed to obtain ℓ. This length scale is then used in a MTEN calculation method, where reasonably accurate results are reported for plane Poiseuille flow and for an axisymmetric jet flow.

Harlow and Nakayama (1969), noting that the length scale will be used to determine the dissipation, proposed a closure model for the exact differential equation for $\mathcal{D}$ derivable from

the Navier-Stokes equations. They experimented with the use of this equation in MTEN closures. The Los Alamos group (private communication) has now abandoned the MTE closure in favor of MRS closures, which also use the $\mathcal{D}$ equation for inference of length scales (see 8.13). They refer to the $\mathcal{D}$ equation as a "dissipation" equation, which as we have noted is not strictly correct.

Hanjalic, Jones and Launder (1970) have used a dissipation model equation to study a variety of boundary layer flows in an extended MTEN model. Their formulation is purported to work in the viscous region, eliminating the need for wall-solution patching (see 8.14).

The interest in and activity with dynamical equations for the dissipation (or length scale) suggests that such equations will shortly become an important and well advertised feature of MTEN prediction methods, and probably of MRS methods as well. The dissipation equation is discussed in greater detail in Section 8.

The boundary layer form of (6.15) is (neglecting viscous terms for the outer region)

$$\left(\frac{\partial}{\partial t} + U_j \frac{\partial}{\partial x_j}\right)q^2/2 = aq^2 \frac{\partial U}{\partial y} - C\frac{q^3}{\ell} - \frac{\partial}{\partial y}(Gq^2 Q_2) \qquad (6.19a)$$

$$a = \pm a_{12} \qquad (6.19b)$$

$$\tau/\rho = -\overline{uv} = aq^2 \qquad (6.19c)$$

Bradshaw, Ferris, and Atwell (1967) use (6.19) to derive a differential equation for the turbulent shear stress τ. The transport velocity Q_2 is taken as $\sqrt{\tau_{max}/\rho}$, where τ_{max} is the maximum value of $\tau(y)$ in the boundary layer. G and ℓ are prescribed as functions of the position across the boundary layer,

and a is essentially taken as constant. Together with (4.10a,b), (6.15) gives a closed set of equations for U , V , and τ ; this system is of <u>hyperbolic</u> type, with three real characteristic lines. Bradshaw, Ferriss and Atwell construct a numerical solution using the method of characteristics; it can also be done using small streamwise steps with an explicit difference scheme (Nash; Wheeler and Johnston private communications). There is a great physical appeal to the characteristics, especially since it is found that the solutions along the outward going characteristic dominates the total solution. This may well be connected with physical observations on the nature of turbulent boundary layers (Kline, et al 1967).

The boundary layer form of (6.14) is (neglecting viscous terms for the outer flow)

$$\left(\frac{\partial}{\partial t} + U_i \frac{\partial}{\partial x_i}\right)\left(\frac{q^2}{2}\right) = \nu_T\left(\frac{\partial U}{\partial y}\right)^2 - C\,\frac{q^3}{\ell} + \frac{\partial}{\partial y}\left[N_Q \nu_T \frac{\partial q^2/2}{\partial y}\right] \qquad (6.20a)$$

$$\nu_T = q\ell F \qquad (6.20b)$$

Then, together with (4.5) and (4.1 a,b) this gives a closed system of equations for U , V , and q , provided C , N_Q , and ℓ are specified. This system is of <u>parabolic</u> type.

Equations (6.19) and (6.20) do not hold in the viscous region near the wall. One must either modify these equations to include viscous effects, or else use special solutions as discussed in Section 4 in this region. Experiments reveal a nearly uniform distribution of q in the wall region, except very close to the wall ($yu^*/\nu<20$) . Moreover, the value of q/u^* seems to be nearly universal, with

$$q \approx 2.5u^* \approx \frac{1}{\kappa}\, u^* \qquad (6.21)$$

This has been used as a "wall" boundary condition for the solution of (6.15) or (6.20).

MH prefer to use equations containing the viscous terms to calculate the inner region directly. Now the manner in which V_{ii} is written and modeled becomes important, and MH's version of the MTEN equation can be written as

$$(\frac{\partial}{\partial t} + U_j \frac{\partial}{\partial x_j})(\frac{q^2}{2}) = 2\nu_T S_{ij} S_{ij} - \frac{q^3}{\ell_\epsilon} + \frac{\partial}{\partial x_j}[(\frac{5}{3}\nu + \nu_T)\frac{\partial q^2/2}{\partial x_j}] \qquad (6.22)$$

The 5/3 factor yielded by MH's treatment of V_{ii} is a main point of the difference with others, and MH's rationale seems most cogent. MH then use a fine mesh near the wall, with ℓ and ℓ_ϵ varying linearly in the wall region, and being uniform in the outer flow. Some of their predictions are discussed in Section 7.

MH also examine MRS closures, and show how the MTEN closure results from the MRS equations with the additional assumption of small departures from isotropy. While this approach is academically interesting, even the most weakly strained flows are far from isotropic (see Champagne, Harris, and Corrsin 1970), and hence the main selling point for MTE methods is that they work very well for predicting a wide class of turbulent shear flows. Examples are given in the following section.

MTE boundary layer equations require the same upstream information as for MVF computations, plus the upstream distribution and free-stream distribution of q. Normally the free-stream turbulence is set zero, but the effect of non-zero free-stream turbulence can be incorporated in a MTE calculation. If a dynamical equation for the length scale is used, then the upstream, free-stream, and wall boundary conditions for ℓ must be given. The

upstream ℓ distribution can be drawn using the ideas in Section 4. At the boundary layer edge $\partial\ell/\partial y = 0$ seems appropriate. In the wall region $\ell = 0$ if the calculation is carried to the wall, and $\ell = \kappa y$ if the mesh computation is patched to a wall region solution at the innermost mesh point. The need for this turbulence information makes MTE methods somewhat more difficult to use, but the ability of a good MTE method to predict more severe test flows may make the extra effort worthwhile.

In the so-called "log" region of turbulent boundary layers, the turbulence energy is essentially determined by a delicate balance between the production and dissipation terms in (6.2). With $q = u^*/\kappa$ and $\ell = \kappa y$ (see 4.8, 6.21) a balance between the first two terms on the right in (6.19a) gives

$$\frac{dU}{dy} = \left(\frac{C}{a\kappa}\right) \frac{u^*}{\kappa y} \tag{6.23}$$

while for (6.20) one has

$$\frac{dU}{dy} = \left(\sqrt{\frac{C}{F\kappa^2}}\right) \frac{u^*}{\kappa y} \tag{6.24}$$

Hence, both models will give the proper logarithmic velocity profile (4.12), provided the parenthetical coefficients are unity in each case.

Heat transfer predictions made using MTEN closures have employed the models described in Section 4. The hydrodynamic calculation yields ν_T, and (4.20) is then used in (4.18) to construct the temperature field.

7. MTE Calculation Examples

The MTES approach has been advocated by Bradshaw and his coworkers (Bradshaw, Ferriss, and Atwell 1967, Bradshaw et al 1966 et seq.). Their predictions for TBLPC must be judged among the very best. The agility of Bradshaw's MTES method to predict severe flows was demonstrated at TBLPC by their results for the Tillmann ledge flow, a boundary layer flow immediately downstream of a turbulent reattachment point (judged the most difficult TBLPC flow). Fig. 15 shows their predictions at a point downstream in this flow, including results for two drastically different initial shear stress distributions. Note that the predictions are very insensitive to the initial (upstream) shear stress distribution. In spite of the modest disparity between the measured and predicted velocity profiles, the predicted momentum thickness and skin friction were in considerably better agreement with the data than were the MTEN and MVF predictions. Indeed, one left TBLPC with the feeling that Bradshaw and Ferriss' MTES method was likely to be the wave of the future.

Nash (1970) has used a combination of Bradshaw's MTES ideas and a Newtonian assumption to treat three-dimensional turbulent boundary layers. Nash takes Bradshaw's structural assumption for the <u>total</u> shear stress vector,

$$\sqrt{(\overline{uv})^2 + (\overline{wv})^2} = aq^2 \qquad (7.1)$$

but then uses the Newtonian approximation

$$\frac{\overline{uv}}{\overline{uw}} = \frac{\partial U/\partial y}{\partial W/\partial z} \qquad (7.2)$$

which assumes alignment of the shear stress and strain rate vectors. The evidence is clear that (7.2) does not hold, yet it fortunately is worst in flows with strong spanwise pressure

gradients, where the pressure gradients and not the shear stress control the mean velocity field. In Fig. 8 we show Wheeler and Johnston's (unpublished) calculation for the boundary layer along a plane of symmetry approaching an obstacle. The integral parameter predictions by MH's MVFN method, Nash's MTES/N method, and Bradshaw's MTES method are almost identical. Nash's (1970) own calculation for a point off of the symmetry plane in a similar flow is shown in Fig. 16. Mellor (1968) made a similar calculation with his MVFN method with comparable results.

Bradshaw (TBLPC-1) himself extended his MTES method to three-dimension boundary layers, using the basic ideas to propose model equations for the vector sum and ratios of the two primary stresses, $\overline{-uv}$ and $\overline{-wv}$. Johnston (1970) has compared the result of predictions by this method with his own data for an infinite swept flow. In particular, data show that the stress vector does not align with the strain-rate vector as the Newtonian closures assume. Hopefully Bradshaw's structural model would work better on this flow but Johnston's calculation shows that the angle of the shear stress vector is predicted quite poorly, although the mean velocity is predicted quite well. It is unlikely that MTE methods will ever predict this structural difference well, and one might hope that MRS methods will do considerably better.

Mc Donald and his associates (unpublished) have developed a MTES method following the lines of their integral method (TBLPC-1), and are using this method in a variety of boundary layer flows. They are also treating boundary layers using the full equations in order to study boundary layers near separation.

There has been considerable activity with MTEN computations. Beckwith and Bushnell (TBLPC-1) presented partial results from their MTEN method at TBLPC, and have since continued with its development. Spalding and his associates pushed ahead with MTES

program development. MH have added to the theoretical framework through their application of the method of matched expansions to the selection of the length scale distribution functions, and by showing how the MTEN equations arise as a limiting case of MRS equations for nearly isotropic turbulence.

The ability of MTEN calculations to accurately predict the mean velocity field and turbulence kinetic energy distribution is demonstrated by Figs. 17 from MH's TBLPC contribution. Their use of a fine computational mesh near the wall is reflected in their accurate prediction of the inner regions.

The MH MTEN predictions at TBLPC were among the best; we again note that these predictions were identical with those of their MVF method for all but one TBLPC flow. Hence, for flows not too rapidly shocked by changes in free-stream or wall conditions, consistent MVF and MTE treatments may be expected to yield nearly the same results for the mean velocity and integral parameters. Of course, only the MTE calculation yields the turbulence energy distribution directly. Fig. 18 shows a MH MTEN calculation for a boundary layer responding to a sudden removal of adverse pressure gradient. Five years ago this would have been regarded as a "difficult" test flow, but we see that MTEN methods now handle it reasonably well.

The ability of MTEN methods to handle sudden changes in boundary conditions is evidenced by recent (unpublished) calculations by Kays and his coworkers (see Loyd, Moffat, and Kays 1970). They have modified an early Spalding MTEN program to the point where it successfully predicts the heat transfer behavior of incompressible turbulent boundary layers with strong pressure gradients and with wall suction or blowing. With sudden changes in pressure gradient or blowing the heat transfer coefficient (Stanton number) changes rapidly, and such calculations are more difficult for MVF methods.

For boundary layers the pressure gradient is conveniently represented by the parameter

$$K = \frac{\nu}{U_\infty^2} \frac{dU_\infty}{dx} \qquad (7.3)$$

Fig. 19 shows a prediction by Kays (unpublished) of the heat transfer to a boundary layer undergoing strong acceleration followed by a relaxation to zero pressure gradient. Note that the sudden jump in Stanton number as the acceleration is removed is predicted quite well. Fig. 20 shows another Kays calculation for an accelerated boundary layer, with blowing beginning midway through the accelerated region and continuing through the relaxation to zero pressure gradient. Fig. 21 shows a prediction for an accelerated boundary layer with blowing, with transpiration terminated upstream of the removal of acceleration. The remarkable success of these calculations suggests that MTEN methods are now developed to the point of utility as tools for engineering analysis.

The MTE methods include a calculation of the turbulence energy, and hence one may study the effects of variable free stream turbulence. Kearney, et. al. (1970) have compared such predictions with their data, and Fig. 22 shows a typical result for strongly accelerated turbulent boundary layer.

The MTEN methods have been applied to free shear flows to a limited degree by Spalding and his coworkers. Fig. 23 shows predictions by Rodi and Spalding (1970) for the asymptotic plane jet. This calculation was made using their model equation for the turbulence length scale. Gosman et al (1969) have documented the Spalding MTEN program in detail, and advocate its application to heat and mass transfer in recirculating flows. Readers should be aware that such programs are under continual development, which should not prevent their use in engineering analysis.

8. MRS Closures

In order to compute the structure of the turbulence (i.e. the R_{ij}), one must employ the dynamical equations for the R_{ij} (6.1). This has been the subject of considerable recent interest, though only a few computational experiments have been carried out and a truly "universal" general theory has yet to be established. We can expect considerable activity on this front, and review the current status here with this in mind.

The problem is again to set up a satisfactory closure structure for the unknown terms in the dynamical equations, here the equations for R_{ij} . Some variation in approach is already evident, and we may expect some interesting debate on the choices over the next several years.

Examination of (6.1) shows that the R_{ij} equations contain a pressure-strain-rate correlation term that vanishes in the contraction (6.2). The effect of this term must therefore be to transfer energy conservatively between the three components R_{11} , R_{22} , and R_{33} , and it is generally believed that this transfer tends to produce isotropy in the turbulent motions. Modelings of this term should incorporate this feature. A plausible model of this term (Rotta 1951), supported somewhat by the data of Champagne, Harris, and Corrsin (1970) is,

$$P_{ij} = \overline{\frac{p}{\rho}\left(\frac{\partial u_i}{\partial x_j} + \frac{\partial u_j}{\partial x_i}\right)} = C \frac{q}{\ell} \left(\frac{q^2}{3} \delta_{ij} - R_{ij}\right) \qquad (8.1)$$

An objection to this model rests on the observation that the fluctuating pressure field is given by a Poisson equation,

$$\frac{1}{\rho} \frac{\partial^2 p}{\partial x_i \partial x_i} = \frac{\partial^2}{\partial x_j \partial x_j} \left[\overline{u_i u_j} - u_i u_j - U_i u_j - U_j u_i\right] \qquad (8.2)$$

This suggests that the P_{ij} model should contain terms arising from interactions between the mean and fluctuating velocities, and should somehow reflect the dependence of the pressure fluctuations on distant velocity fluctuations. Daly and Harlow (1970, hereafter referred to as DH) have attempted to include these effects in a complex closure approximation still in an experimental stage (see 9.8a). Other MRS closure calculations have all used (8.1). Some new suggestions are explored in Section 9.

The pressure-velocity terms have been modeled in all MRS computations of which I am aware by extensions of the gradient diffusion model (6.8). Donaldson and Rosenbaum (1968, hereafter referred to as DR) use

$$\frac{1}{\rho}\overline{pu_i} = -q\ell_\epsilon \frac{\partial R_{ik}}{\partial x_k} \tag{8.3}$$

DH use a similar expression with a more complex coefficient. MH suggest

$$\frac{1}{\rho}\overline{pu_i} = -\frac{1}{3} q\ell_P \frac{\partial q^2}{\partial x_i} \tag{8.4}$$

Various forms of gradient diffusion models have been suggested for the triple velocity term. DR use and MH accept

$$\overline{u_i u_j u_k} = -q\ell_d \left(\frac{\partial R_{ij}}{\partial x_k} + \frac{\partial R_{jk}}{\partial x_i} + \frac{\partial R_{ki}}{\partial x_j}\right) \tag{8.5}$$

The DH representation may be cast as

$$\overline{u_i u_j u_k} = -C \frac{\ell_\epsilon}{q} \frac{\partial R_{ij}}{\partial x_m} R_{km} \tag{8.6}$$

If the objections to a gradient-diffusion approach are valid, one should presumably use an extension of (6.9). A possible large-eddy transport model is

$$\overline{u_i u_j u_k} = R_{ij}Q_k + R_{ik}Q_j + R_{jk}Q_i \tag{8.7}$$

The viscous terms have also been handled in different ways. DR and DH use V_{ij} in the form (6.3). Following Glushko (1965), DR take

$$D_{ij} \equiv \frac{1}{2}\overline{\frac{\partial u_i}{\partial x_k}\frac{\partial u_j}{\partial x_k}} = \frac{1}{2}\frac{R_{ij}}{\ell_D^2} \tag{8.8}$$

DH put

$$D_{ij} = \frac{2D}{q^2}R_{ij} \tag{8.9}$$

and use another differential equation for $D \equiv D_{ii} = \mathcal{D}/2\nu$. MH, invoking arguments of local isotropy and using kinetic theory as a guide, propose using (6.5) with

$$\overline{u_i \sigma_{kj}} + \overline{u_j \sigma_{ki}} = \frac{\partial R_{jk}}{\partial x_i} + \frac{\partial R_{ik}}{\partial x_j} + \frac{\partial R_{ij}}{\partial x_k} \tag{8.10}$$

and

$$\nu\,\overline{\left[\sigma_{jk}\frac{\partial u_i}{\partial x_k} + \sigma_{ik}\frac{\partial u_j}{\partial x_k}\right]} = \frac{2}{3}\frac{q^3}{\ell_\epsilon}\delta_{ij} \tag{8.11}$$

In order to complete the closure, the various length scales in the models above must be prescribed or related to the other independent variables through a differential equation. DH use a dynamical equation for $\mathcal{D}$, derived exactly from the Navier-Stokes equations and then closed by assumptions. The $\mathcal{D}$ equation will be discussed shortly. DH are now considering the use of two

length scale equations for the dissipating and energy containing eddies.

MH have given considerable thought to the MRS closure, and show how the MTEN equations emerge from MRS equations if it is assumed that the turbulence structure is nearly isotropic.

Calculations with MRS closure models have been carried out by DR, DH, and Harlow and Romero (1969). Harlow and Romero used the model with moderate success to study the distortion of isotropic turbulent (see Section 9). DR considered plane turbulent boundary layer flow in zero pressure gradient, and specified what seem to be reasonable length scale distributions for this calculation. DR's prediction of the mean velocity profile is good (but not better than a good MVF or MTE calculation); their predicted turbulent stress distributions, shown in Fig. 24 are in substantial agreement with experiments. DH studied plane Poiseuille flow with a more complex model, obtaining less satisfactory results. The DH model is not accurate near the wall, and is currently undergoing further extension and adjustment. Hirt (1969) gives a useful summary of the thinking behind developments in the Los Alamos group.

Let's now consider the "dissipation" transport equation. The dynamical equation for $\mathscr{D}$ is derived by differentiating the momentum equation for u_i with respect to x_j, multiplying by $2\nu\partial u_i/\partial x_j$ and averaging. The result is

$$\frac{\partial \mathcal{E}}{\partial t} + U_j \frac{\partial \mathcal{E}}{\partial x_j} = \nu \frac{\partial^2 \mathcal{E}}{\partial x_j \partial x_j} - 2\nu \Bigg\{ \frac{\partial^2 U_j}{\partial x_i \partial x_k} \overline{\left(u_k \frac{\partial u_j}{\partial x_i}\right)}$$

$$+ \frac{\partial U_j}{\partial x_k} \overline{\left(\frac{\partial u_j}{\partial x_i} \frac{\partial u_k}{\partial x_i}\right)} + \frac{\partial U_k}{\partial x_i} \overline{\left(\frac{\partial u_j}{\partial x_i} \frac{\partial u_j}{\partial x_k}\right)}$$

$$+ \overline{\frac{\partial u_j}{\partial x_i} \frac{\partial u_k}{\partial x_i} \frac{\partial u_j}{\partial x_k}} + \frac{1}{2} \frac{\partial}{\partial x_k} \left(\overline{u_k \frac{\partial u_j}{\partial x_i} \frac{\partial u_j}{\partial x_i}} \right)$$

$$+ \frac{\partial}{\partial x_j} \overline{\left(\frac{\partial u_j}{\partial x_i} \frac{\partial p}{\partial x_i}\right)} + \nu \overline{\left(\frac{\partial^2 u_j}{\partial x_k \partial x_i} \frac{\partial^2 u_j}{\partial x_k \partial x_i}\right)} \Bigg\} \qquad (8.12)$$

Now, to obtain closure one must propose models of all the terms between the braces on the right hand side of (8.12). This requires a considerable amount of courage as well as insight; there is no direct experimental evidence about any of the terms, and one can really only conjecture as to their effect. Lumley (1970) has used some rational reasoning for the special case of homogeneous flows (Section 9). DH used some qualitative ideas about the effect of each term and proposed a model of (8.12), viz.

$$\frac{\partial \mathcal{E}}{\partial t} + U_j \frac{\partial \mathcal{E}}{\partial X_j} = \frac{\partial}{\partial x_j} \left(\nu + \frac{2q^2}{\mathcal{E}} R_{jk}\right) \frac{\partial \mathcal{E}}{\partial x_k} - b_1 \frac{\mathcal{E}}{q^2} R_{jk} \frac{\partial U_j}{\partial x_k}$$

$$+ \frac{\mathcal{E}}{q^2} \frac{\partial}{\partial x_j} \left(\frac{2q^2}{\mathcal{E}} R_{jk} \frac{\partial q^2/2}{\partial x_k}\right)$$

$$+ b_2 \frac{\partial}{\partial x_j} \left(q^2 \frac{\partial R_{jk}}{\partial x_k}\right) - F \frac{\mathcal{E}^2}{q^2} \qquad (8.13)$$

Here b_1 and b_2 are "universal parameters, all with values near unity (or possibly equal to zero)", and F is a function

of the turbulence Reynolds number. DH also in effect make the assumption that $\mathscr{D} = \epsilon$ through their treatment of the R_{ii} equation.

Hanjalic, Jones, and Launder (1970) propose a model of (8.12) which can be generalized as

$$\frac{\partial \mathscr{D}}{\partial t} + U_j \frac{\partial \mathscr{D}}{\partial x_j} = \frac{\partial}{\partial x_i}\left[(\nu + N_S \nu_T)\frac{\partial \mathscr{D}}{\partial x_j}\right] + c_1 \frac{\mathscr{D}}{q^2}\nu_T S_{ij} S_{ij}$$

$$-c_2 f_2 \frac{\mathscr{D}^2}{q^2} + f_3 \nu \nu_T \left(\frac{\partial^2 U_i}{\partial x_j \partial x_j}\frac{\partial^2 U_i}{\partial x_k \partial x_k}\right) \qquad (8.14)$$

Here c_1 and c_2 are constants, and f_1, f_2, and f_3 are functions of the turbulence Reynolds number. They report that "encouraging" results are obtained when this equation is used in an MTEN computational scheme. Clearly the use of such equations is presently quite experimental, and (8.14) is given here to illustrate the rather substantial differences in ideas as to how best to model (8.12).

For the special case of homogeneous flows at high turbulence Reynolds numbers (8.13) and (8.14) do have a common form. Both may be written as

$$\frac{\partial \mathscr{D}}{\partial t} + U_j \frac{\partial \mathscr{D}}{\partial x_j} = -C_1 \frac{\mathscr{D}^2}{q^2} + C_2 \frac{\mathscr{D}\mathscr{P}}{q^2} \qquad (8.15)$$

where $\mathscr{P}$ is the rate of production of turbulence energy. This form is probably quite adequate for homogeneous flows (Section 9).

Lumley (1970) has studied the distortion of homogeneous turbulence by uniform strain using a limited MRS closure. In homogeneous flow the R_{ij} equations become

$$\frac{dR_{ij}}{dt} = - R_{ik} \frac{\partial U_j}{\partial x_k} - R_{jk} \frac{\partial U_i}{\partial x_k} - \frac{1}{\rho} \overline{\left(u_j \frac{\partial p}{\partial x_i} + u_i \frac{\partial p}{\partial x_j}\right)}$$

$$- 2\nu \overline{\frac{\partial u_i}{\partial x_j} \frac{\partial u_i}{\partial x_j}} \qquad (8.16)$$

Lumley closes by taking

$$\nu \overline{\frac{\partial u_i}{\partial x_k} \frac{\partial u_j}{\partial x_k}} = \epsilon \frac{\delta_{ij}}{3} \qquad (8.17)$$

$$- \frac{1}{\rho} \overline{\left(u_j \frac{\partial p}{\partial x_i} + u_i \frac{\partial p}{\partial x_j}\right)} = \frac{1}{T} \left(q^2 \frac{\delta_{ij}}{3} - R_{ij}\right) \qquad (8.18)$$

where T is a time scale of the turbulence (compare 8.1). He further assumes that the time scale is related to the dissipation rate by

$$T = \frac{C_1 q^2}{2\epsilon} \qquad (8.19)$$

which is equivalent to (6.6). The dissipation rate is in turn described by

$$\frac{d\epsilon}{dt} = - 4 \frac{\epsilon^2}{q^2} \qquad (8.20)$$

as deduced by Lumley from scaling arguments based on (8.12) (compare 8.15).

Lumley has solved the equation system for homogeneous shear, and compared the results with homogeneous strain and homogeneous shear experiments. Lumley's model predicts that the time scale T grows without bound, so that homogeneous flows can never attain an equilibrium structure. Champagne, Harris, and Corrsin's (1970)

experiments are consistent with Lumley's notion, but Lumley's model does not predict the observed structure very well. Some improvements on Lumley's model based on (8.15) are suggested in Section 9.

It does seem clear that equilibrium is never obtained in homogeneous flows. In inhomogeneous flows the transport features apparently act to set the equilibrium structure. MTES methods really shouldn't work in homogeneous flows, and we might well be suspicious of methods when the "universal constants" are obtained by tests against such flows.

9. Some New Ideas for Homogeneous Flows

It became apparent in preparing this review that too little attention has been given to systematic development of the closure model. The approach has been to construct a comprehensive model, with numerous universal constants, and then to select these constants by optimizing the average fit to a number of selected flows. A more systematic approach would be to develop the closure model in a step-by-step approach, working gradually through a heirarchy of experimental flows.

In order to develop some feeling for what might be accomplished, I examined the following approximations to homogeneous flow:

(1) Decay of isotropic turbulence (Townsend 1956)

(2) Return to isotropy in the absence of strain or shear (Tucker and Reynolds 1968, hereafter referred to as TR)

(3) Development of structure under pure strain (TR)

(4) Development of structure under pure shear (Champagne, Harris, and Corrsin 1970, hereafter referred to as CHC).

The starting point of this analysis was the dynamical equations for the turbulent kinetic energy and the dissipation. For homogeneous flows these equations are

$$\frac{dq^2/2}{dt} = \mathcal{P} - \epsilon \qquad (9.1)$$

$$\frac{d\varepsilon}{dt} = - C_1 \frac{\varepsilon^2}{q^2} + C_2 \frac{\mathcal{P}\varepsilon}{q^2} \qquad (9.2)$$

Here $\mathcal{P} = -R_{ij}S_{ij}$ is the rate of turbulence energy production. Equation (9.1) is exact, and (9.2) is the form in which the dissipation equations of DH, Hanjalic, Jones and Launder (1970), and the length scale equation of Ng and Spalding (1970) can be expressed (see 8.15). For very weakly strained flows, Lumley (1970) developed the C_1 term with $C_1 = 4$ from first principles, and neglected the C_2 terms in his weak strain model (8.20). Hanjalic et al suggest $C_1 = 4$ and $C_2 = 3.2$. Ng and Spalding's empirical flow fitting is equivalent to $C_1 = 3.9$ and $C_2 = 3.3$. DH use $C_1 = 4$ and $C_2 = 2$.

If one considers the decay of homogeneous isotropic turbulence with zero strain for large turbulence Reynolds numbers, and models the dissipation by

$$\varepsilon = q^3/\ell \qquad (9.3)$$

(9.1) and (9.2) produce

$$\frac{dq^2/2}{dt} = - \frac{q^3}{(C_1-3)\ell} \qquad (9.4)$$

$$\frac{d\ell}{dt} = (C_1-3)q \qquad (9.5)$$

Now, experiments indicate that $q^2 \sim t^{-1}$, $\ell \sim t$ which requires $C_1 = 4$. This seems a clear choice.

To investigate C_2 I calculated the distribution of $\mathcal{P}$ from the data of CHC, and carefully determined an initial value for ε from the experimental q^2 distribution (taking the starting point at $x = 5$ ft in their experiments). The differential equations

(9.1) and (9.2) were then solved numerically for different values of C_2 ; $C_2 = 2$ is clearly preferred (Fig. 25a,b). A similar calculation was carried out for the TR flow (Fig. 26a), where $C_2 = 2$ also gives excellent agreement. Note that the predicted length scale variations model the integral scale changes as measured by CHC (Fig 25b). It therefore appears that a satisfactory model equation for the dissipation history in homogeneous flows is

$$\frac{d\epsilon}{dt} = - 4 \frac{\epsilon^2}{q^2} + 2 \frac{\epsilon \mathcal{P}}{q^2} \qquad (9.6)$$

Next I considered the R_{ij} equations with the objective of obtaining a model that, with (9.11) and (9.6), correctly predicts the measured R_{ij} . Closure assumptions are required for the pressure strain and dissipation term. In all calculations I took (6.5) and (8.11) in (6.1), and hence wrote

$$\frac{dR_{ij}}{dt} = - R_{ik} \frac{\partial U_j}{\partial x_k} - R_{jk} \frac{\partial U_i}{\partial x_k} + P_{ij} - \frac{2}{3} \epsilon \delta_{ij} \qquad (9.7a)$$

where the pressure-strain term is

$$P_{ij} = \overline{\frac{p}{\rho} \left(\frac{\partial u_i}{\partial x_j} + \frac{\partial u_j}{\partial x_i}\right)} \qquad (9.7b)$$

I first took

$$P_{ij} = C_3 \epsilon \left(\frac{1}{3} \delta_{ij} - R_{ij}/q^2\right) \qquad (9.8)$$

The first test was for the strain-free portion of the TR flow, where the structure is relaxing towards isotropy. Calculations showed that $C_3 = 5$ gives a good representation of the structure, energy, and production in this flow (Fig. 26b).

I then proceeded to try (9.8) with $C_3 = 5$ in the straining regions of the TR and CHC flows, but was not satisfied with the energy predictions (see Figs. 25c,d,26c,d). It appears that some alteration in either the P_{ij} or dissipation terms is required, and I chose to experiment with modifications in the P_{ij}. A ground rule was that proposed modification could not alter what has already been systematically established. The forms investigated were

$$P_{ij} = (5\epsilon + C_4\mathcal{P})(\tfrac{1}{3}\delta_{ij} - \frac{R_{ij}}{q^2}) \tag{9.9a}$$

$$P_{ij} = 5\epsilon\ (\tfrac{1}{3}\ \delta_{ij} - \frac{R_{ij}}{q^2}) + C_4 q^2 S_{ij} \tag{9.9b}$$

$$P_{ij} = 5\epsilon\ (\tfrac{1}{3}\ \delta_{ij} - \frac{R_{ij}}{q^2}) + C_4(R_{ik}S_{kj} + R_{jk}S_{ki} + \tfrac{2}{3}\mathcal{P}\ \delta_{ij}) \equiv P_{ij}^* \tag{9.9c}$$

$$P_{ij} = P_{ij}^* + C_5\ [R_{ik}(\frac{\partial U_j}{\partial x_k} - \frac{\partial U_k}{\partial x_j}) + R_{jk}(\frac{\partial U_i}{\partial x_k} - \frac{\partial U_k}{\partial x_i})] \tag{9.9d}$$

Note that $P_{ii} = 0$ in each case. Eq. (9.9a) is DH's form with slightly different constants. Equations (9.9b)-(9.9d) are suggested by the notion that interactions between the mean strain rate and fluctuation fields contribute to the pressure fluctuations. The closures (9.9a) and (9.9b) were unsatisfactory. For the TR flow (9.9c) with $C_4 = 1/2$ works very well (Fig. 26c,d), but it is not adequate for the CHC flow (Fig. 25c,d). Equation (9.9d) reduces to (9.9c) for irrotational mean flow, i.e. the TR flow, and with $C_4 = 1/2$ and $C_5 = 1/4$ (9.9d) predicts the CHC flow reasonably well (Fig. 25c,d).

It does seem clear that (9.7) is not adequate in flows with strain or shear. With the constants indicated, (9.9d) is

$$P_{ij} = 5\epsilon\left(\frac{1}{3}\delta_{ij} - \frac{R_{ij}}{q^2}\right) + \frac{1}{2}(R_{ik}S_{kj} + R_{jk}S_{ki} + \frac{2}{3}\mathcal{P}\delta_{ij})$$

$$+ \frac{1}{4}\left[R_{ik}\left(\frac{\partial U_j}{\partial x_k} - \frac{\partial U_k}{\partial x_j}\right) + R_{jk}\left(\frac{\partial U_i}{\partial x_k} - \frac{\partial U_k}{\partial x_j}\right)\right] \qquad (9.10)$$

which is probably better. Further development is needed, and (9.10) is offered here as an interim model. However, it is not clear that (9.10) is a model of P_{ij} ; it could just as well be a model for its complement (see 8.18) as used by Lumley (1970) in (8.16)!

10. Outlook for the Future

It should not be long before simple boundary layer flows are routinely handled in industry by MVF prediction methods. These methods are easy to use, require a minimum of input data, and give results which are usually adequate for engineering purposes. MTE methods will become increasingly important to both engineers and scientists, for they afford the possibility of including at least some important effects missed by MFV methods. The debate over the gradient-diffusion vs. large-eddy-transport closures will continue, and both methods will probably continue to be used with nearly equal success. MRS methods will be explored from the scientific side, and porbably will not be used to any substantial degree in engineering work for some time to come.

Considerable effort is likely to be expended on the development of length scale (or equivalent) equations, such as the dissipation equation discussed in Section 8. In this connection the two-point correlation

$$\mathcal{R}_{ij} = \overline{u_i(x)u_j(x + \xi)} \tag{10.1}$$

could be used to advantage, either along the lines of Gawain and Pritchard (1970), or perhaps through a closure of its own dynamical equation (Hinze 1959).

This equation will of course involve six independent space variables, but by integration over the separations ξ these variables could be removed. Then, one might assume the form of R_{ij}, say

$$\mathcal{R}_{ij} = R_{ij}\, e^{-\xi_k/\ell_k} \tag{10.2}$$

and carry out the integrations, thereby obtaining three additional differential equations of the transport type relating the integral scales ℓ_i and the one-point correlations (turbulent stresses) R_{ij}. Experimental calculations along these lines would be most interesting.

The heavy computation approach (Deardorff 1970) might be used to numerically test the closure assumptions used in the simpler MRS and MTE models. Hopefully such computations will be documented in the future with this use in mind.

The MRS closures will attract most interest for use where MTE methods fail. For example, in flows with rotation the coriolis terms enter the R_{ij} equations, but drop out in the equation for $R_{ii} = q^2$. Therefore, it probably will be essential to go to a MRS method to include rotation effects, which are of considerable importance in many practical engineering and geophysical problems. Other effects which have not yet been adequately modeled and for which MRS methods may offer some hope include additive drag reduction, ultra-high Reynolds numbers, separation, roughness, lateral and transverse curvature, and strong thermal processes that affect the hydrodynamic motions.

We might also see the complex closure models used as the basis for computationally simpler integral methods. The success of integral methods of this type at TBLPC (MC,HR; TBLPC-1) should not be forgotten in the rush to use the full partial differential equations.

A disappointing aspect of the current status is that very little use has been made of the substantial advances made over the past decade in our understanding of the structure of turbulent shear flows. We know that large eddy structures dominate such flows; only MTES methods recognize this at all, and then not

quantitatively; MTEN methods ignore it all together. MRS calculations have not used the large eddy idea at all. Indeed, the concept of a "transport theory" for turbulent correlations would seem antithetical to a large eddy view. We know that the wall region is dominated by a particular correlatable structure, yet none of the current prediction methods make any use of this fact. The structure of the outer region of boundary layers has been extensively studied recently, and entrainment of non-turbulent fluid through the turbulent interface (superlayer) is known to be a critical process in turbulent shear flows; no real utilization of this fact has been incorporated into any of the closure models. We know that the outer layer flow has a dual structure, intermittently consisting of turbulent and non-turbulent regions with considerably different character. Yet all calculation methods are based on averages taken over long periods of time, averages that wash out this essential feature of the flow. Some believe a similar duality exists in the wall region; might not this also be incorporated?

In short, it seems that too much attention has been paid to the numerical aspects of the computations; indeed, the difficulty of a first encounter with complex differencing schemes has made this necessary. But now we should begin a concerted effort to bring the new physical information into the turbulent flow computation methods, and we look for a better situation ten years hence.

Finally, for those who cannot or choose not to take up the computation game, perhaps some fresh thinking at the fundamental level might be fruitful. For example, we all want to compute turbulent flows. Just what is it that we are working so hard to compute? What is the operational definition of turbulence?

REFERENCES

Bradshaw, P. et al 1966 et seq, Calculation of boundary-layer development using the turbulent energy equation, Natl.Phys. Lab. Aero Div. reports 1182, 1217, 1271, 1286, 1287, 1288

Bradshaw, P., Ferriss, D. H., and Atwell, N. P., 1967 Calculations of boundary layer development using the turbulent energy equation, J. Fluid. Mech., 28, 593

Bradshaw, P., 1970 The use of transport equations for Reynolds stress (to appear).

Busse, F. H., 1970 Bounds for turbulent shear flow, J. Fluid. Mech., 41, 219

Byrne, J. E., and Hatton, A. P., 1970 Prediction and measurement of velocity and temperature profiles in turbulent boundary layers

Cebeci, T., Smith, A.M.O., and Mosinskis, G., 1969 Calculation of compressible adiabatic turbulent boundary layers, AIAA paper 69-687

Cebeci, T., 1970a Application of exact turbulent boundary layer equations as a means of calculating heat and mass transfer in incompressible and compressible flows, Preprints, Fourth International Heat Transfer Conference, Paris.

Cebeci, T., 1970b A model for eddy-conductivity and turbulent Prandtl number, Report MDC-j0747/01, McDonnell Douglas Co.

Champagne, F.H., Harris, V.G., and Corrsin, S., 1970 Experiments on nearly homogeneous turbulent shear flow, J. Fluid. Mech., 41, p 81

Daly, B.J., and Harlow F.H. 1970 Los Alamos Scientific Lab preprint LA-DC-11304 (to appear in Phys. Fluids)

Davis, R.E., 1970 On the turbulent flow over a wavy boundary, J. Fluid Mech. 42, 721

Deardorff, J.W., 1970 A numerical study of three-dimensional turbulent channel flow at large Reynolds numbers, J. Fluid Mech., 41, 453

Donaldson, C.D., and Rosenbaum, H., 1968 Calculation of turbulent shear flows through closure of the Reynolds equations by invariant modeling, Aero Res. Assoc. of Princeton Report 127

Gawain, T.H., and Pritchard, J.W., 1970 A unified Hueristic model of turbulence, J. Comp. Physics., 5, 385

Glushko, G.S., 1965 Turbulent boundary layer on a flat plate in an incompressible fluid, NASA TTF-10,080 (translation of Izv. Akad. Nauk SSSR (Mekhanika), 4, p 13

Gosman, A.D., Pun, W.M., Runchal, A.K., Spalding, D.B., and Wolfshtein, M., 1969 Heat and mass transfer in recirculating flows, Academic Press, London

Hanjalic, K., Jones, W.P., and Launder, B.E., 1970 Some notes on an energy-dissipation model of turbulence, Imperial Col., London (internal report)

Harlow, F.H., and Nakayama, P.I., 1967 Turbulence transport equations, Phys. Fluids 10, 2323

Harlow, F.H., and Romero, N.C., 1969 Turbulence distortion in a nonuniform tunnel, Los Alamos Lab report LA-4247

Harlow, F.H., and Nakayama, P.I., 1969 Los Alamos Scientific Lab preprint LA-DC-8635

Herring, H.J., and Mellor, G.L., 1968 A method of calculating compressible turbulent boundary layers, NASA CR-1444

Hinze, J.O., 1959 Turbulence, McGraw Hill Book Co., Inc.

Hirt, C.W., 1969 Computer studies of time-dependent turbulent flows, Phys. Fluids, 12, II-219

Howard, L.N., 1963 Heat transport by turbulent convection, J. Fluid Mech., 17, 405

Hussain, A.K.M.F., and Reynolds, W.C., 1970 The mechanics of perturbation wave in turbulent shear flow, Report FM-6, Mech. Engrg. Dept., Stanford. See also J. Fluid Mech., 41,241

Johnston, J.P., 1970 Measurements in a three-dimensional turbulent boundary layer induced by a swept, forward facing step, J. Fluid. Mech., 42, 823

Kasahara, A., 1969 Simulation of the earth's atmosphere, Comp. Approaches in App. Mech., ASME

Kearney, D. et al 1970 The effect of free-stream turbulence on heat transfer to strongly accelerated turbulent boundary layers, Proc. 1970 Heat Transfer and Fluid Mech. Institute, Stanford U. Press

Kendall, J.M., 1970 The turbulent boundary layer over a wall with progressive surface waves, J. Fluid Mech. 41,

Kline, S. J. et al 1967 The structure of turbulent boundary layers, J. Fluid Mech., 30, 741

Lighthill, M. J., 1952, Reviews, J. Fluid Mech., 1, 554

Loyd, R.J., Moffat, R.J., and Kays, W.M., 1970 The turbulent boundary layer on a porous plate; an experimental study of the fluid dynamics with strong favorable pressure gradients and blowing, Report HMT-13, Mech. Engrg. Dept., Stanford U.

Lumley, J.L., 1970, Toward a turbulent constitutive equation, J. Fluid Mech., 41, p. 413

Lundgren, T. S., 1967 Distribution functions in the statistical theory of turbulence, Phys. Fluids, 10, 969

Mellor, G. L., 1967 Incompressible turbulent boundary layers with arbitrary pressure gradients and divergent or convergent cross flows, AIAA Jour., 5, 1570

Mellor, G.L., and Herring, H.J., 1970a,b, A study of turbulent boundary layer models (a) Part I, (b) Part II, Sandia Lab. Report SC-CR-70-6125.

Nash, J.F., 1970 The calculation of three-dimensional turbulent boundary layers in incompressible flow, J.Fluid Mech., 37, 625

Ng, K.H., and Spalding, D.B., Some applications of a model of turbulence for boundary layers near walls (to appear in Phys. Fluids--see also Imperial Col. report B1/TN/14, Aug. 1969)

Patankar, S.V., and Spalding, D.S., 1967 Heat and Mass Transfer in Boundary Layers, C.R.C. press, Cleveland. See also Int. J. Heat and Mass Trans., 10, 1389

Prandtl, L. 1945 Nach. Akad. Wiss. Gottengem, Math-pysile, K. 1 ("On a new representation of fully developed turbulence", JPL Publication No. 13 (1952), trans. by. D. Coles)

Rotta, J.C., 1951 Zeitschrift fur Physik, I: 129,547-752; II: 131, 51-77

Russell, B., 1961, A History of Western Philosophy, Allen and Unwin, London

Simpson, R.L., Whitten, D.G., and Moffat, R.J., 1970 An experimental study of the turbulent Prandtl number of air with injection and suction, Int. J. Heat Mass Trans., 13, 125

Spalding, D.B., and Rodi, 1970 A two-parameter model of turbulence and its application to free jets, Warme-und Stuffubertragung, 3, 85.

Stewart, R.H., 1970 Laboratory studies of the velocity field over deep water waves, J. Fluid Mech., 42, 733

TBLPC 1968 Proceedings - Computation of Turbulent Boundary Layers-1968 AFOSR-IFP - Stanford Conference; Vol. 1 (Ed. Kline et al) Methods, predictions, evaluation and flow structure; Vol. 2 (Ed. Coles and Hirst) Compiled data; Thermosciences Div., Dept. of Mech. Engrg., Stanford U., Stanford, Ca. 94305.

Townsend, A.A., 1956 The structure of turbulent shear flow, Cambridge U. Press

Tucker, H.J., and Reynolds, A.J., 1968 The distortion of turbulence by irrotational plain strain, J. Fluid Mech. 32, 657

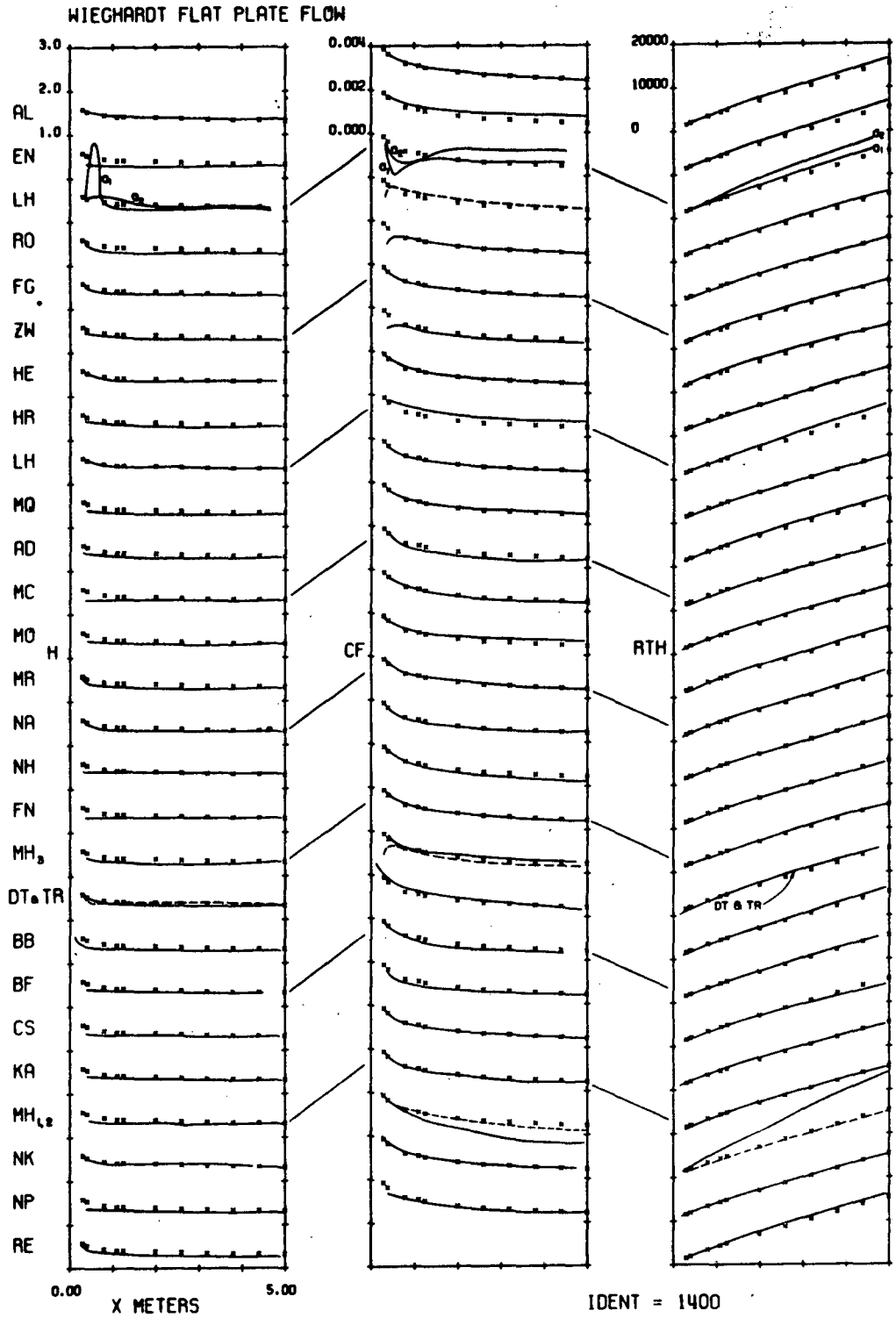
WIEGHARDT FLAT PLATE FLOW
3.0
2.0
1.0
AL
EN
LH
RO
FG
ZW
HE
HR
LH
MQ
AD
MC
MO
MR
NA
NH
FN
MH3
DT&TR
BB
BF
CS
KA
MH12
NK
NP
RE
H
0.004
0.002
0.000
CF
20000
10000
0
RTH
DT & TR
0.00
5.00
X METERS
IDENT = 1400

FIG. 1

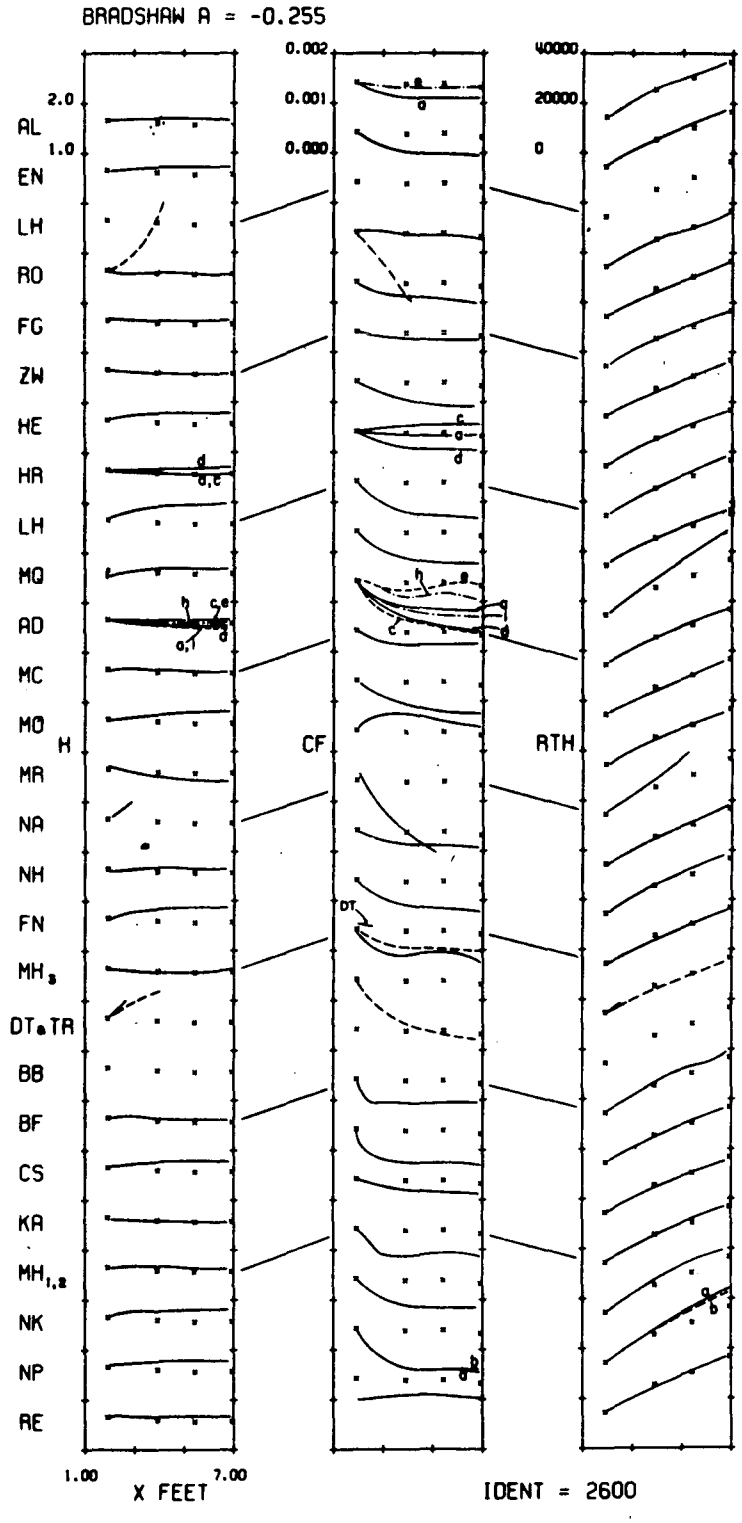
BRADSHAW A = -0.255
2.0
AL
1.0
EN
LH
RO
FG
ZW
HE
HR
LH
MQ
AD
MC
MO
H
MR
NA
NH
FN
MH3
DT&TR
BB
BF
CS
KA
MH1,2
NK
NP
RE
0.002
0.001
0.000
CF
DT
40000
20000
0
RTH
1.00
X FEET
7.00
IDENT = 2600

FIG. 2

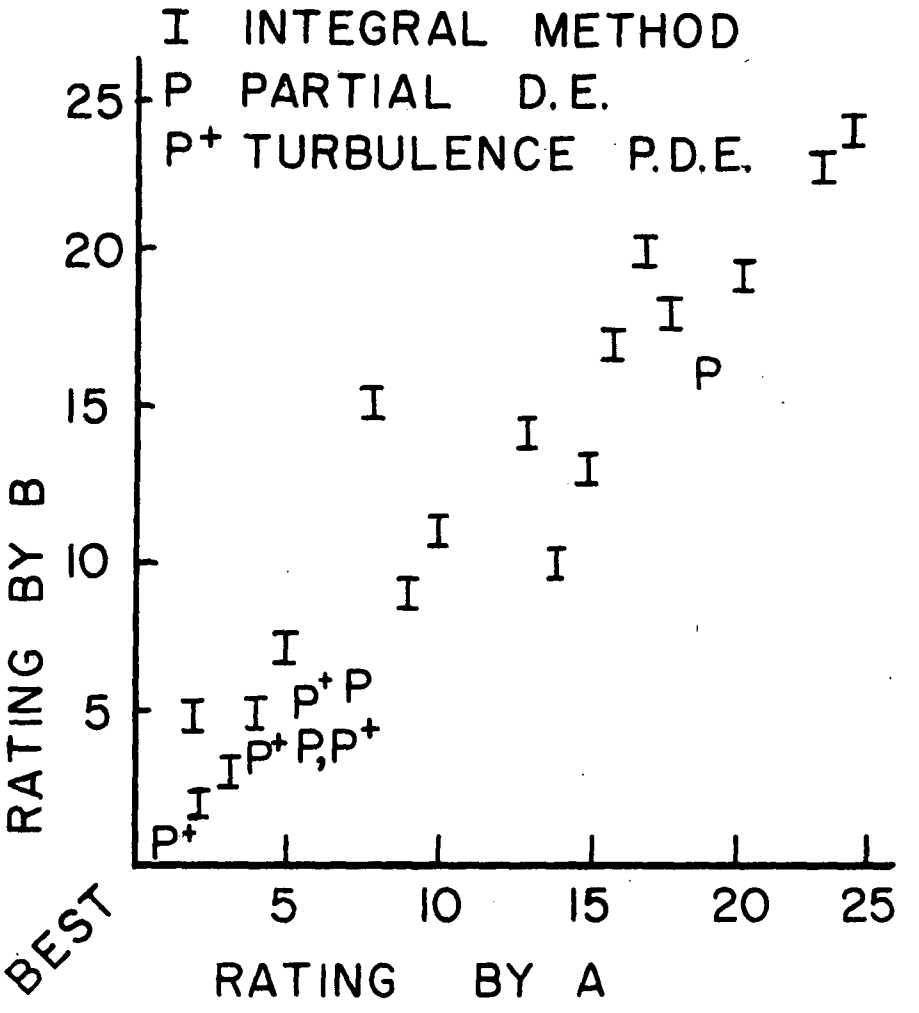
I INTEGRAL METHOD
P PARTIAL D.E.
P+ TURBULENCE P.D.E.
RATING BY B
BEST
RATING BY A
5
10
15
20
25

FIG. 3

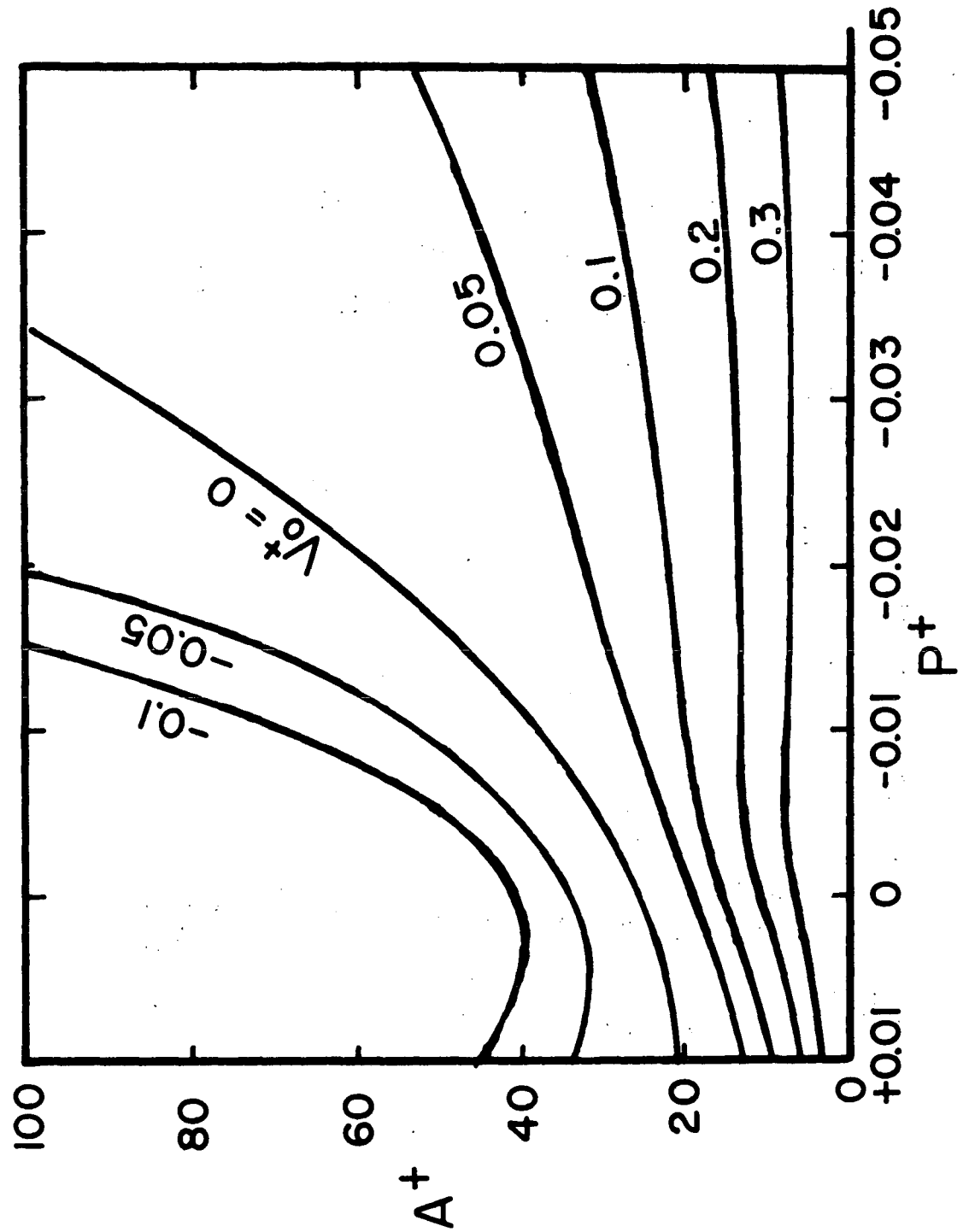
100
80
60
40
20
0
+0.01
0
-0.01
-0.02
-0.03
-0.04
-0.05
A^+
p^+
0.05
0.1
0.2
0.3
$V_0^+ = 0$
-0.05
-0.1

FIG. 4

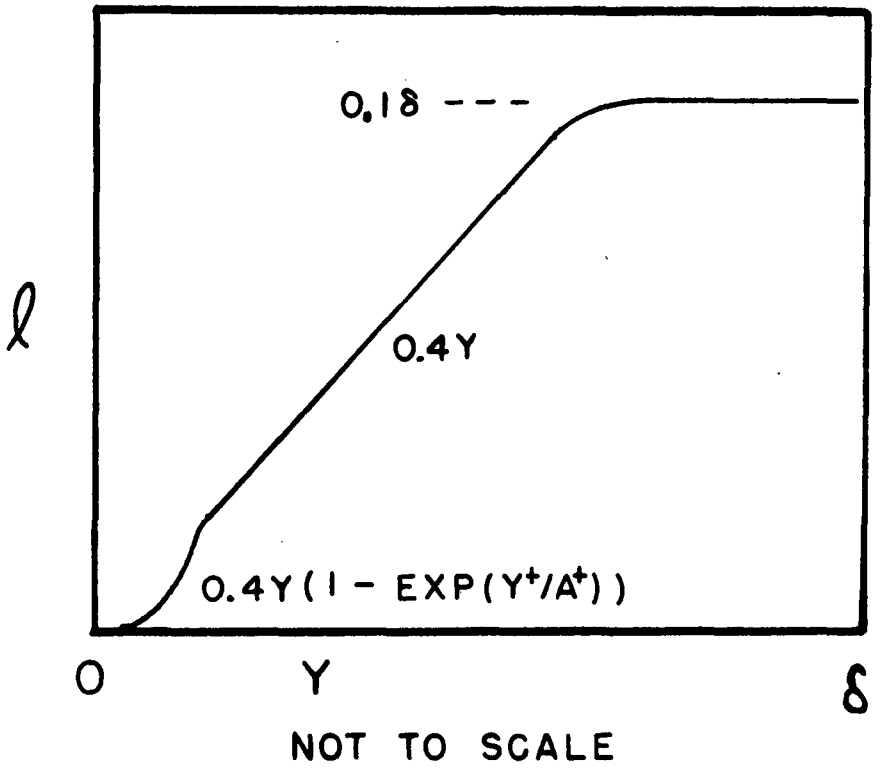

FIG. 5

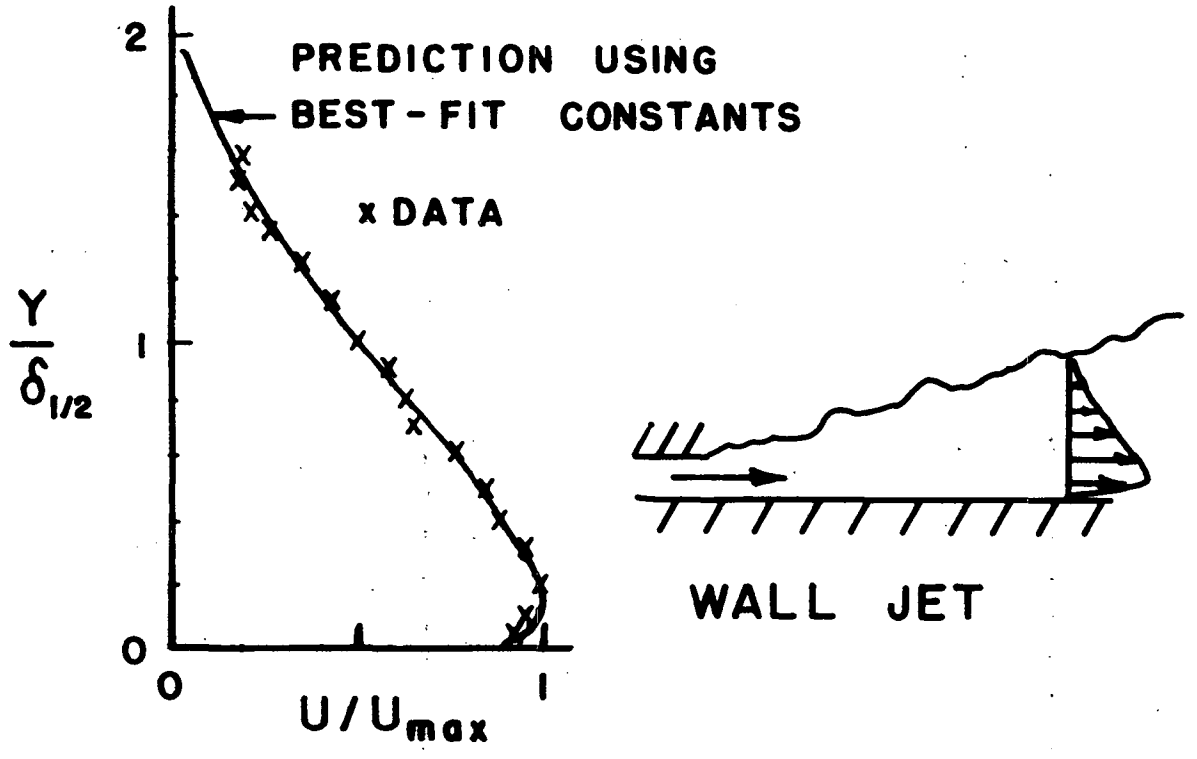
PREDICTION USING
BEST-FIT CONSTANTS
x DATA
Y/δ1/2
2
1
0
0
1
U/Umax
WALL JET

FIG. 6

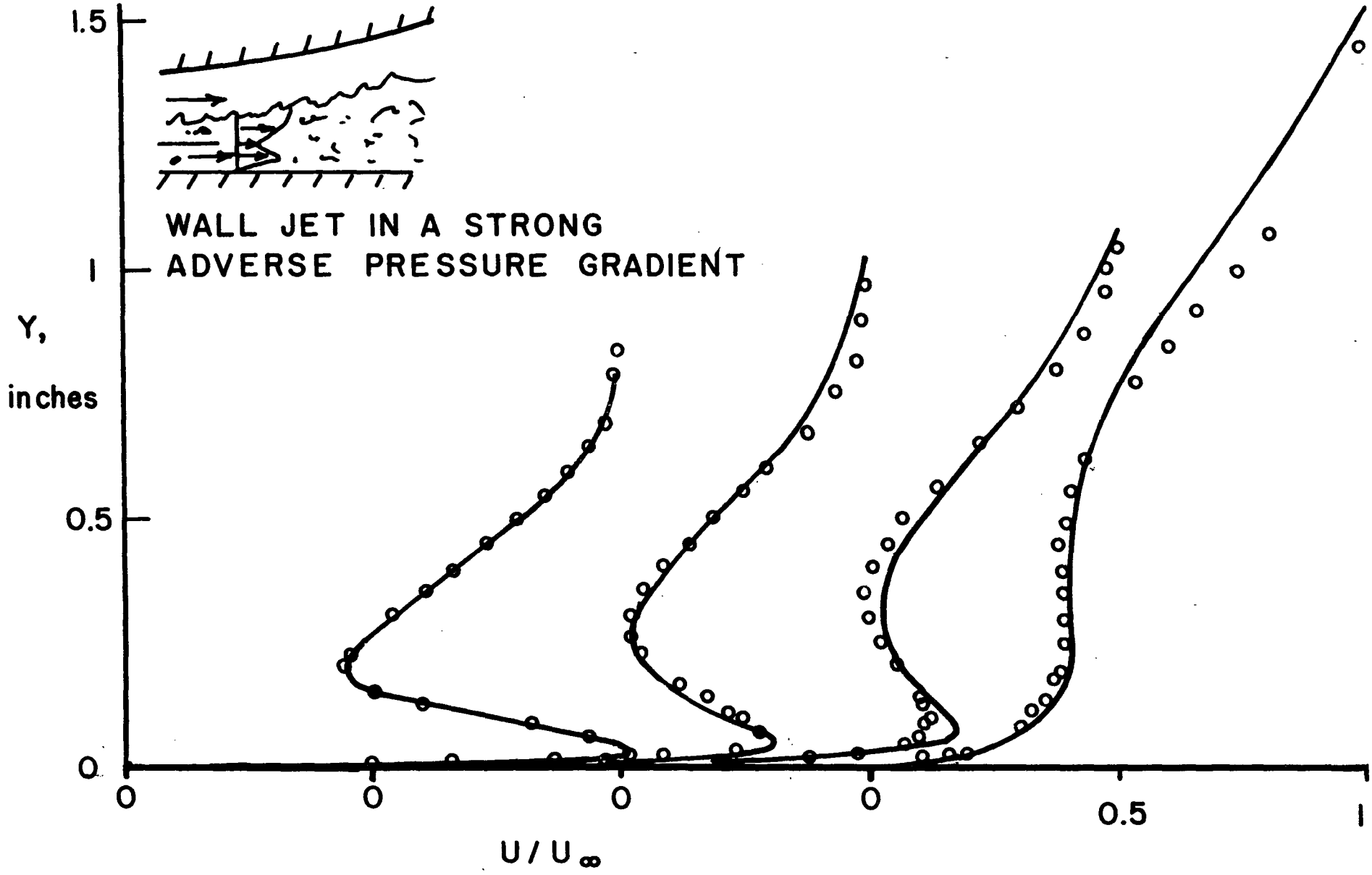
WALL JET IN A STRONG
ADVERSE PRESSURE GRADIENT
1.5
1
0.5
0
Y,
inches
0
0
0
0
0.5
1
U / U∞

FIG. 7

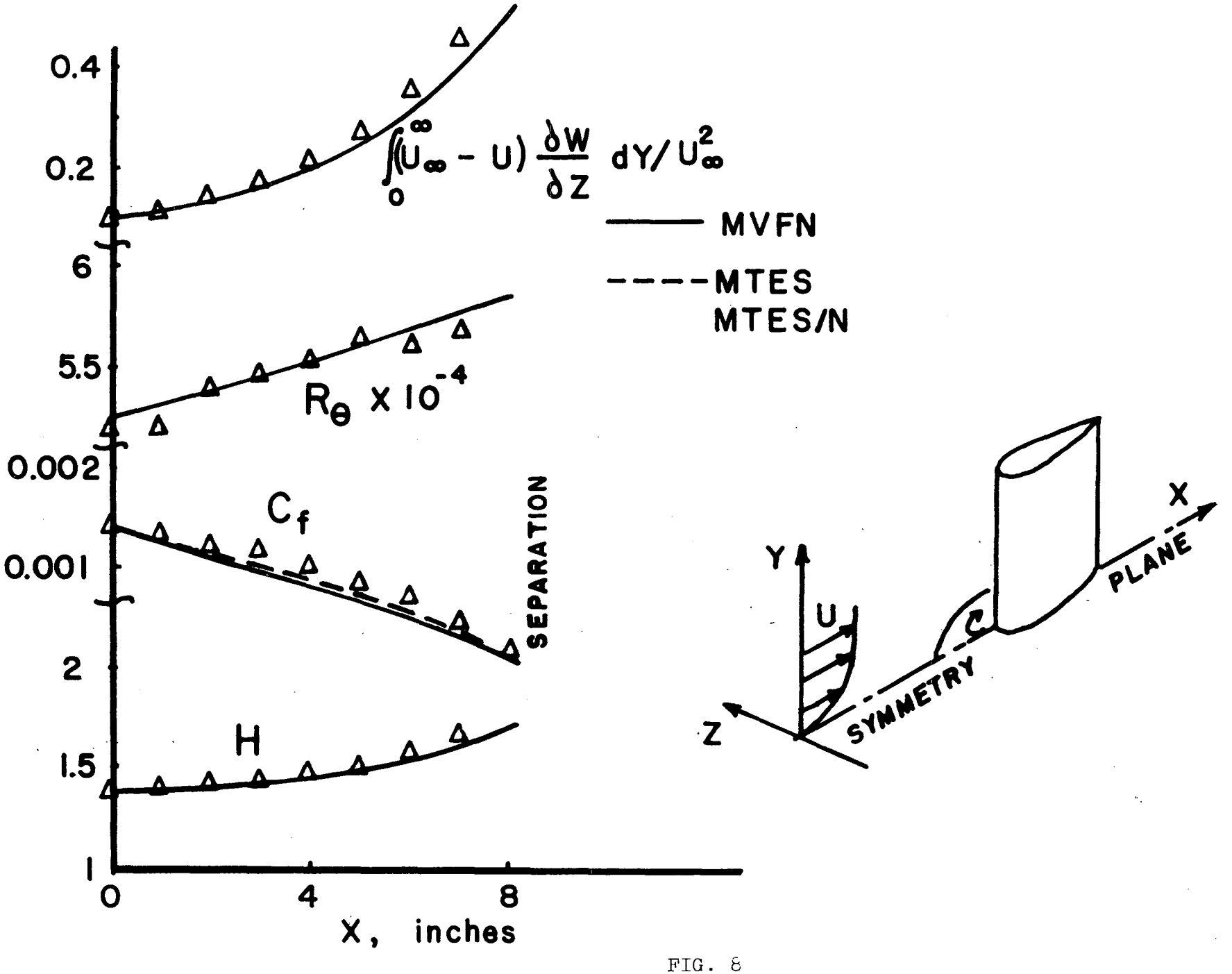
0.4
0.2
6
5.5
0.002
0.001
2
1.5
1
0
4
8
X, inches
$\int_0^\infty (U_\infty - U)\frac{\delta W}{\delta Z}\, dY / U_\infty^2$
MVFN
MTES
MTES/N
$R_\theta \times 10^{-4}$
C_f
H
SEPARATION
Y
U
Z
X
PLANE
SYMMETRY

FIG. 8

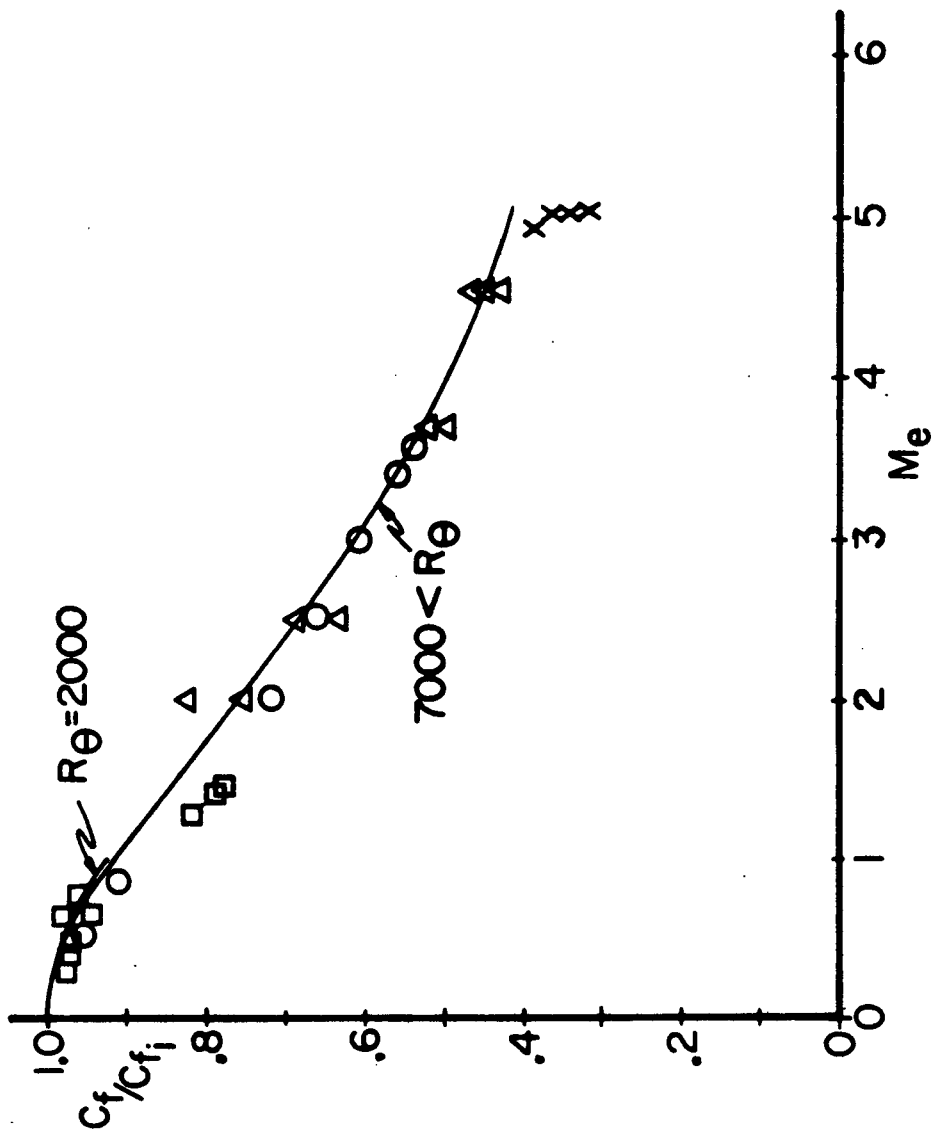

FIG. 9

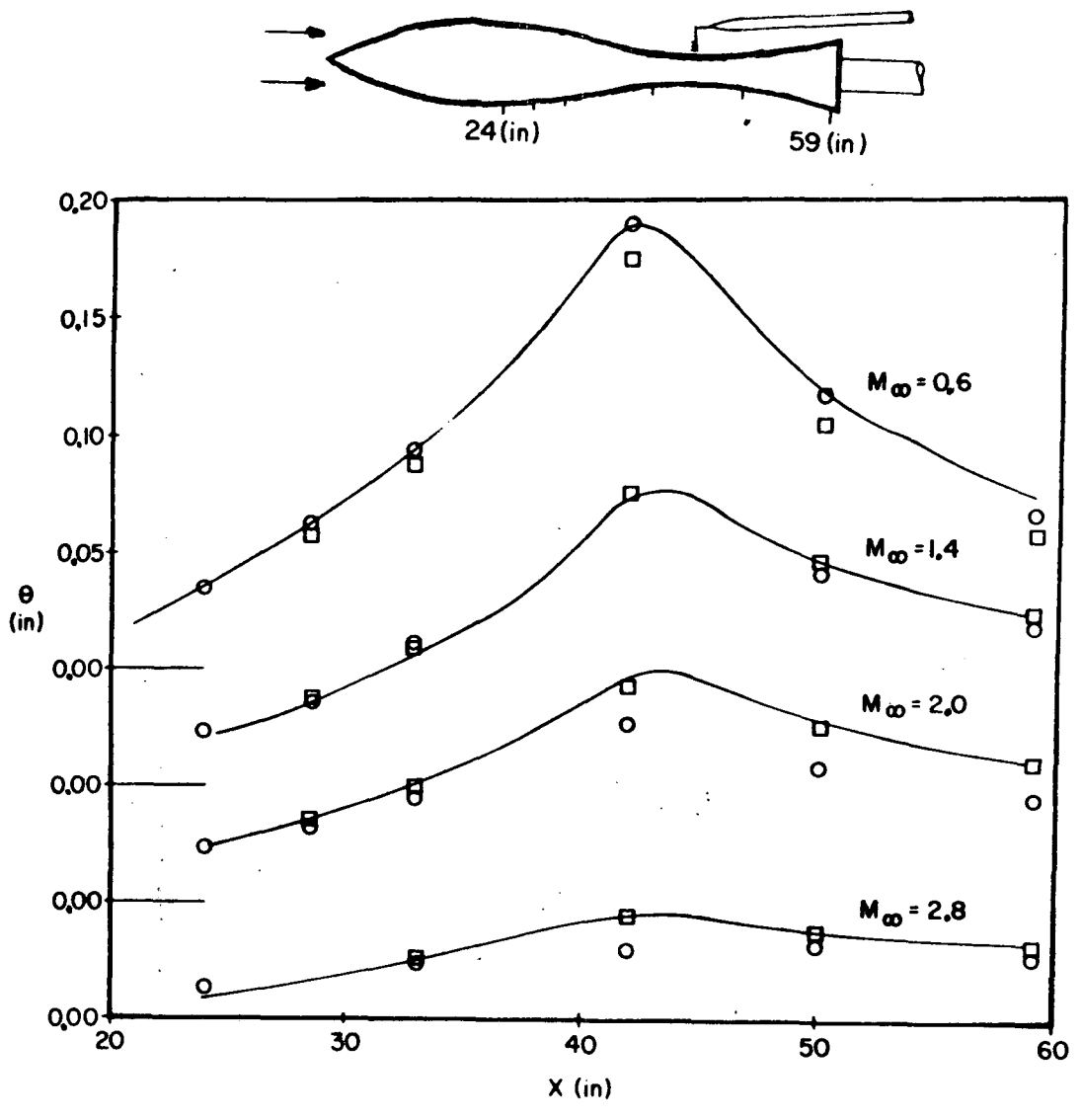
24 (in)
59 (in)
0.20
0.15
0.10
0.05
θ (in)
0.00
0.00
0.00
0.00
$M_\infty = 0.6$
$M_\infty = 1.4$
$M_\infty = 2.0$
$M_\infty = 2.8$
20
30
40
50
60
X (in)

FIG. 10a

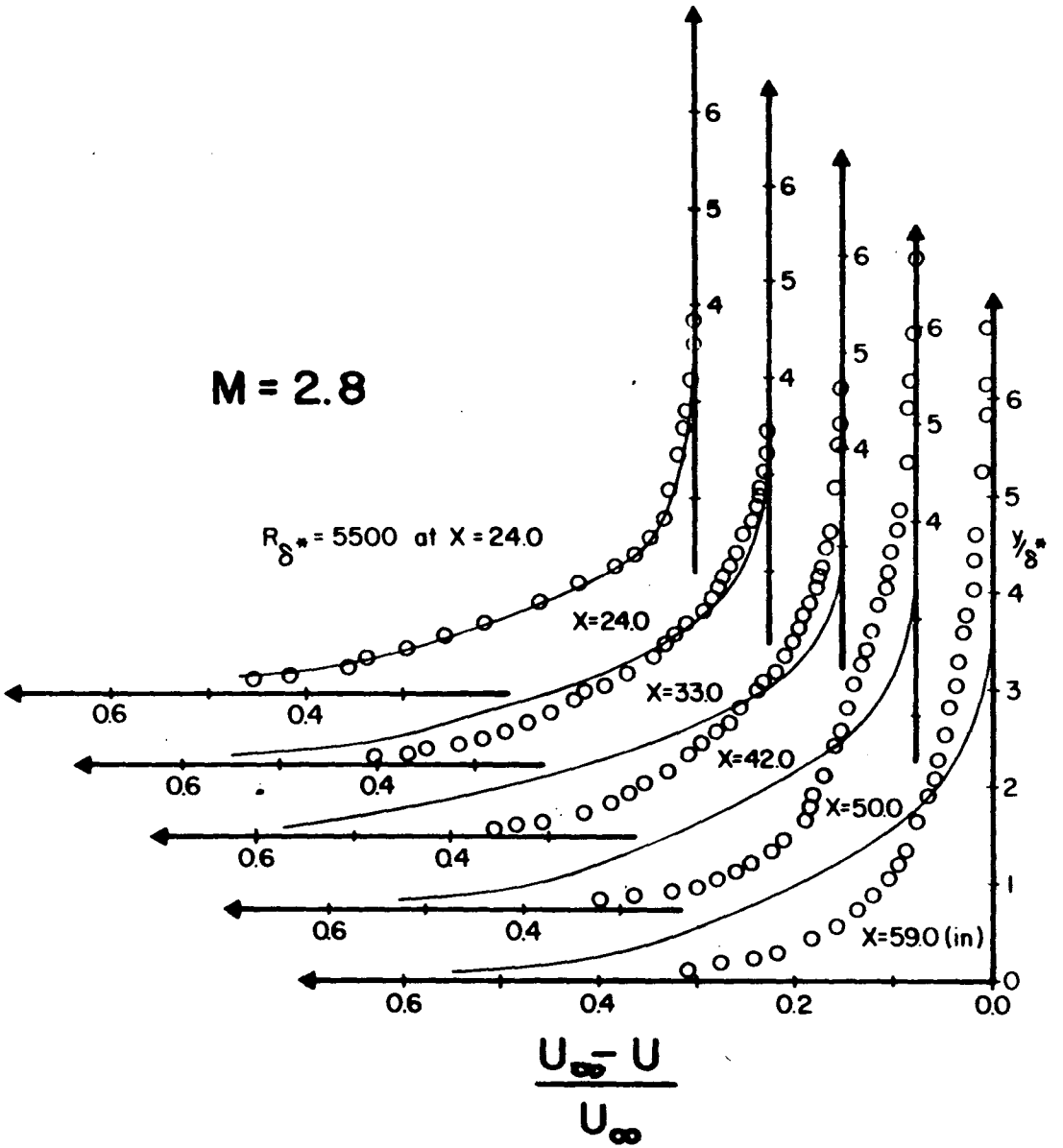
M = 2.8
R_{δ^*} = 5500 at X = 24.0
X=24.0
X=33.0
X=42.0
X=50.0
X=59.0 (in)
0.6
0.4
0.2
0.0
$\frac{U_\infty - U}{U_\infty}$
y/δ^*
0
1
2
3
4
5
6

FIG. 10b

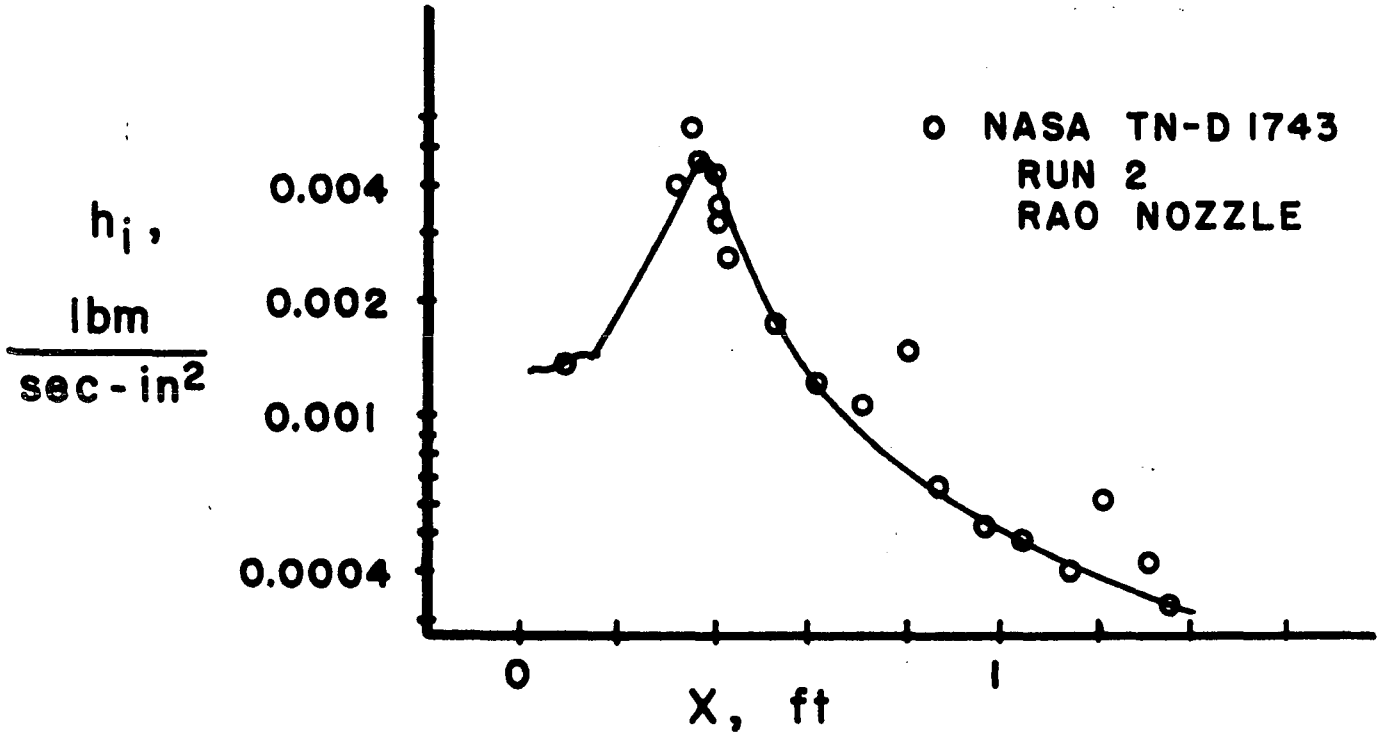
h_i, lbm / sec-in^2
0.004
0.002
0.001
0.0004
0
1
X, ft
NASA TN-D 1743
RUN 2
RAO NOZZLE

FIG. 11

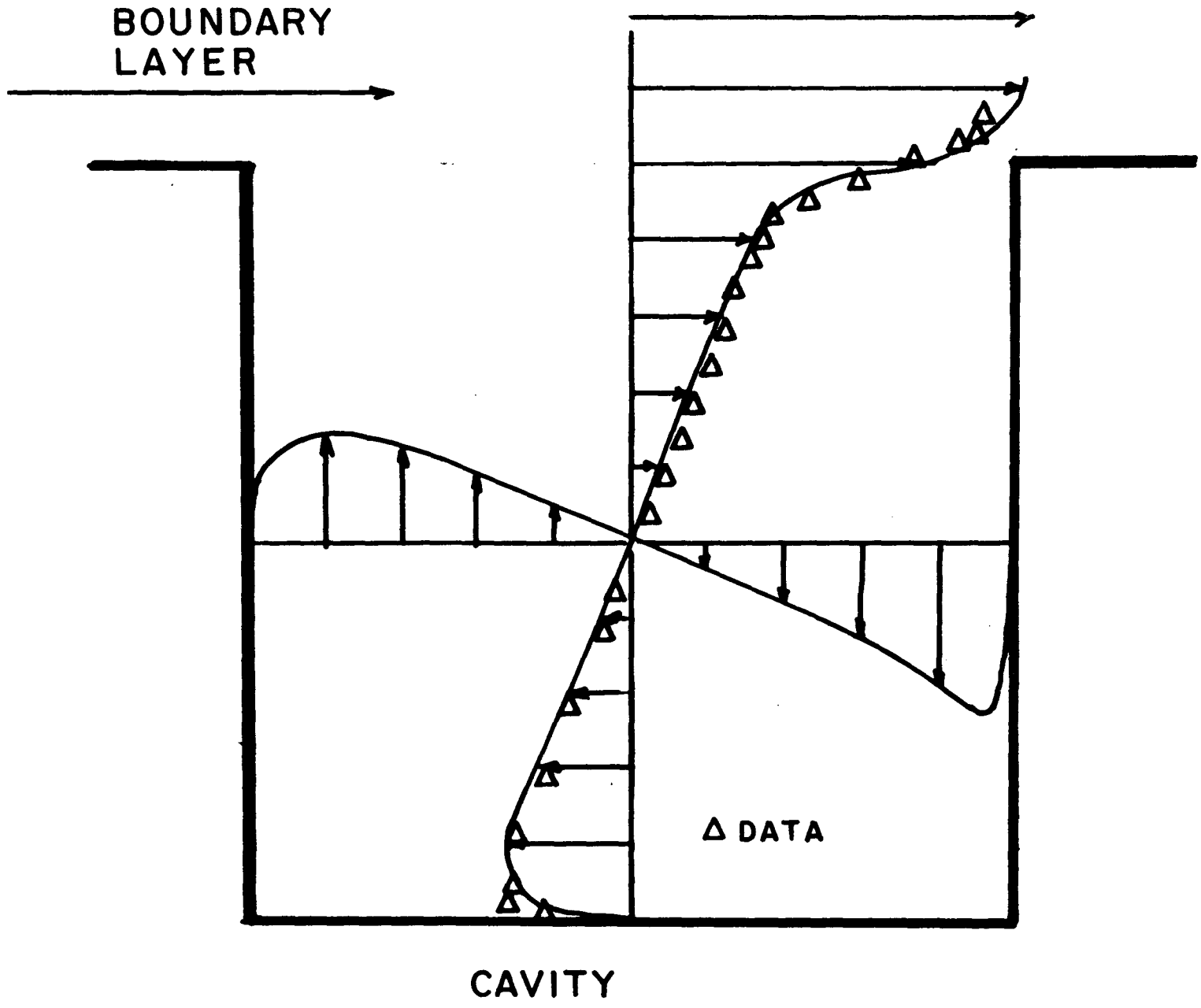

FIG. 12

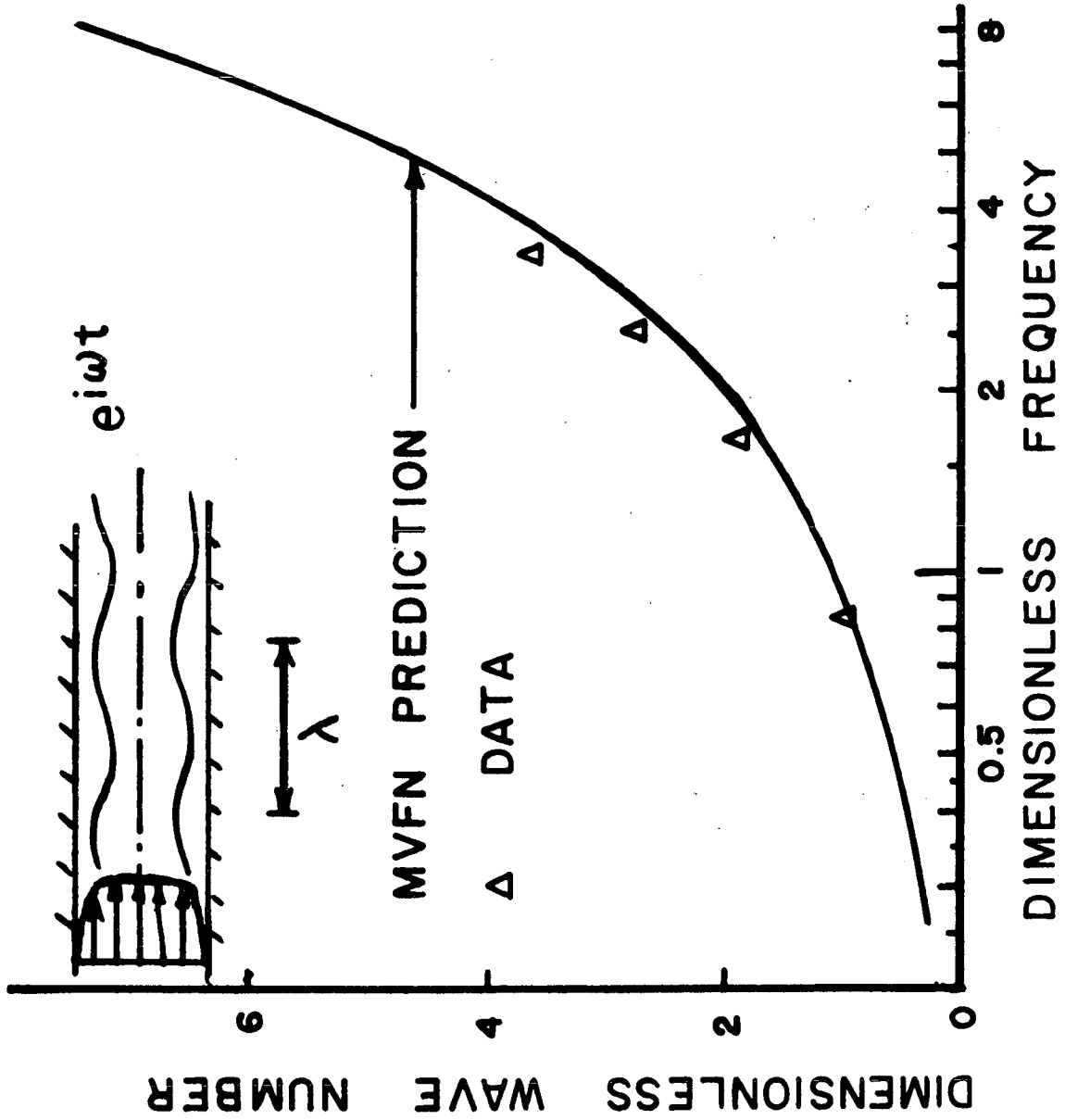
DIMENSIONLESS WAVE NUMBER
0
2
4
6
DIMENSIONLESS FREQUENCY
0.5
1
2
4
8
MVFN PREDICTION
DATA
λ
eiωt

FIG. 13

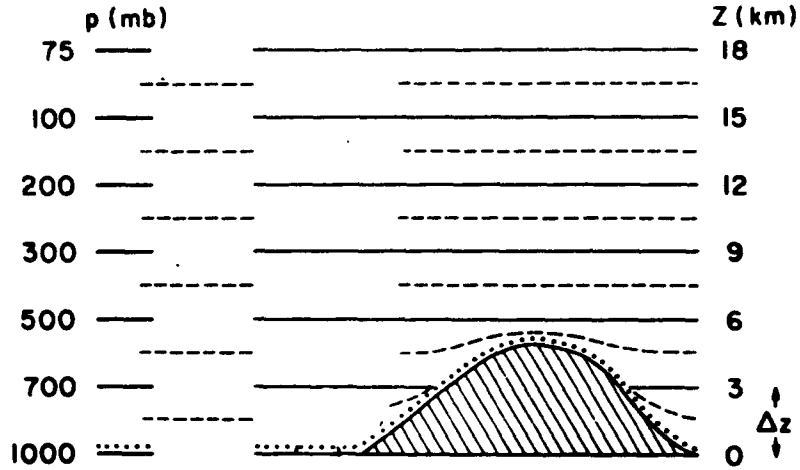
p (mb)
Z (km)
75
100
200
300
500
700
1000
18
15
12
9
6
3
0
Δz

(a)

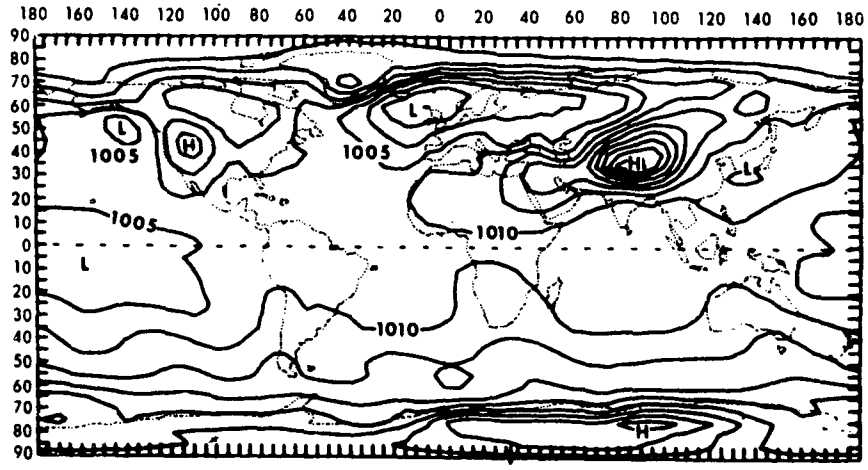
180 160 140 120 100 80 60 40 20 0 20 40 60 80 100 120 140 160 180
90 80 70 60 50 40 30 20 10 0 10 20 30 40 50 60 70 80 90
L
H
1005
1010
HI

(b)

FIGS. 14a, b

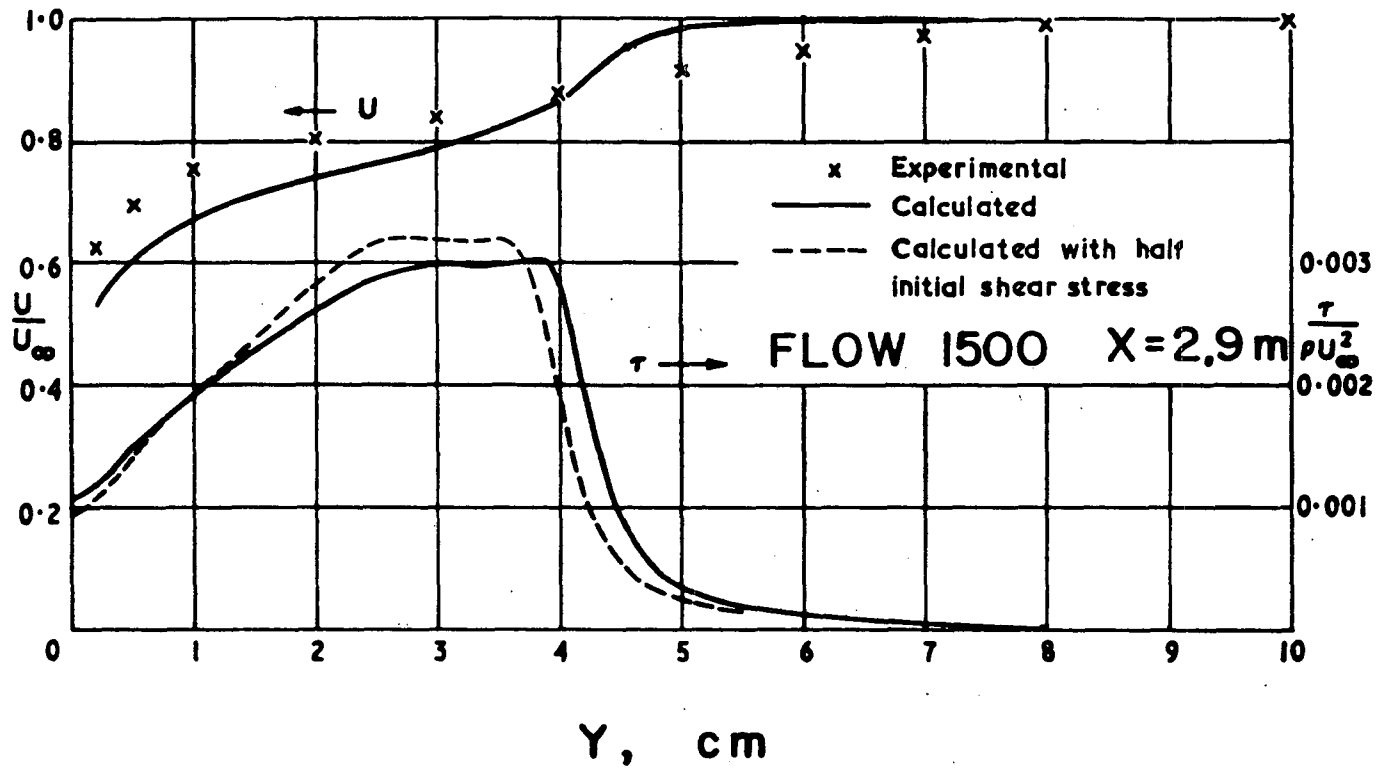
1·0
0·8
0·6
0·4
0·2
0
U/U∞
U
x Experimental
Calculated
Calculated with half initial shear stress
τ
FLOW 1500 X=2,9 m
0·003
0·002
0·001
τ/ρU∞²
1
2
3
4
5
6
7
8
9
10
Y, cm

FIG. 15

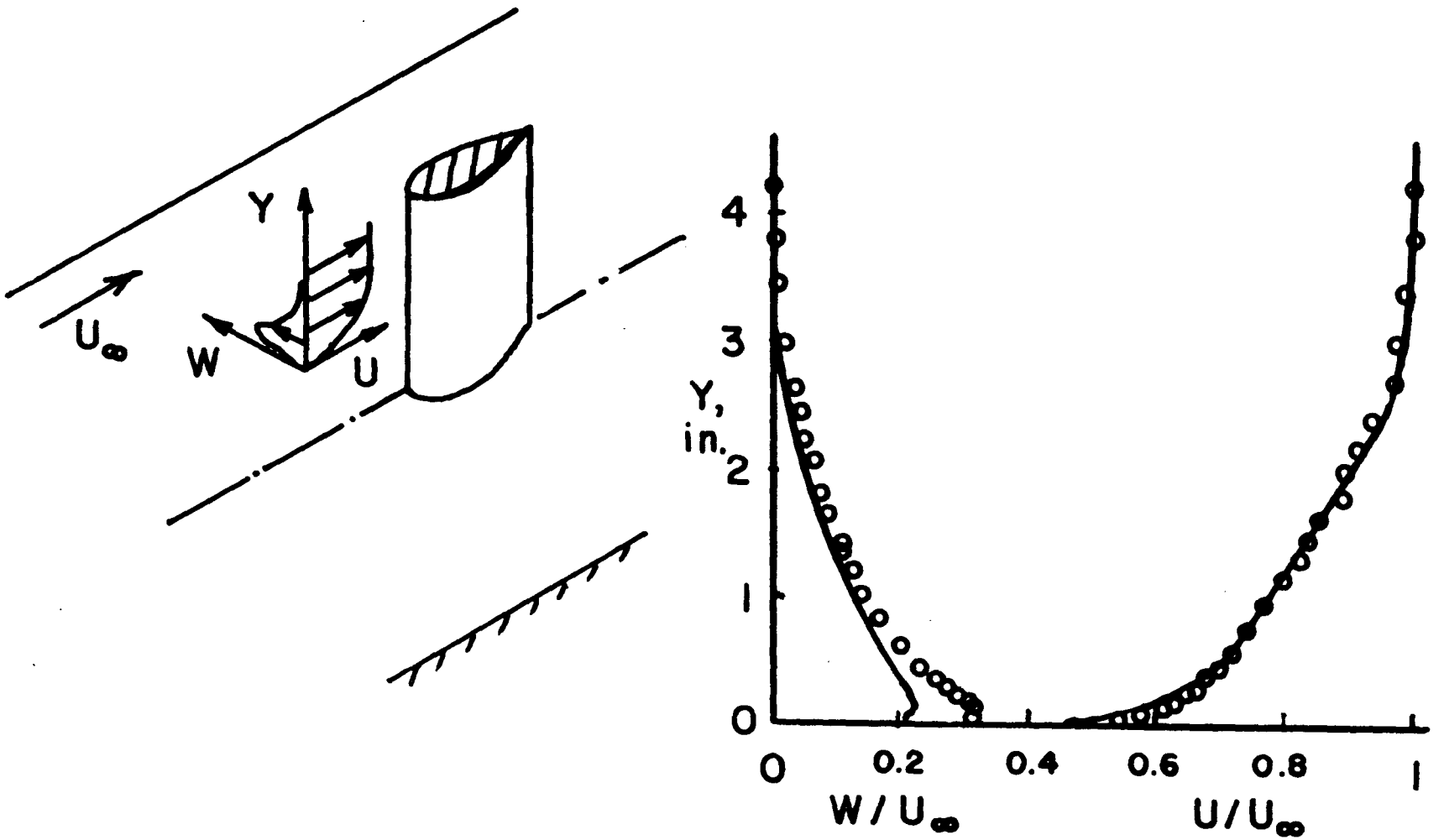

FIG. 16

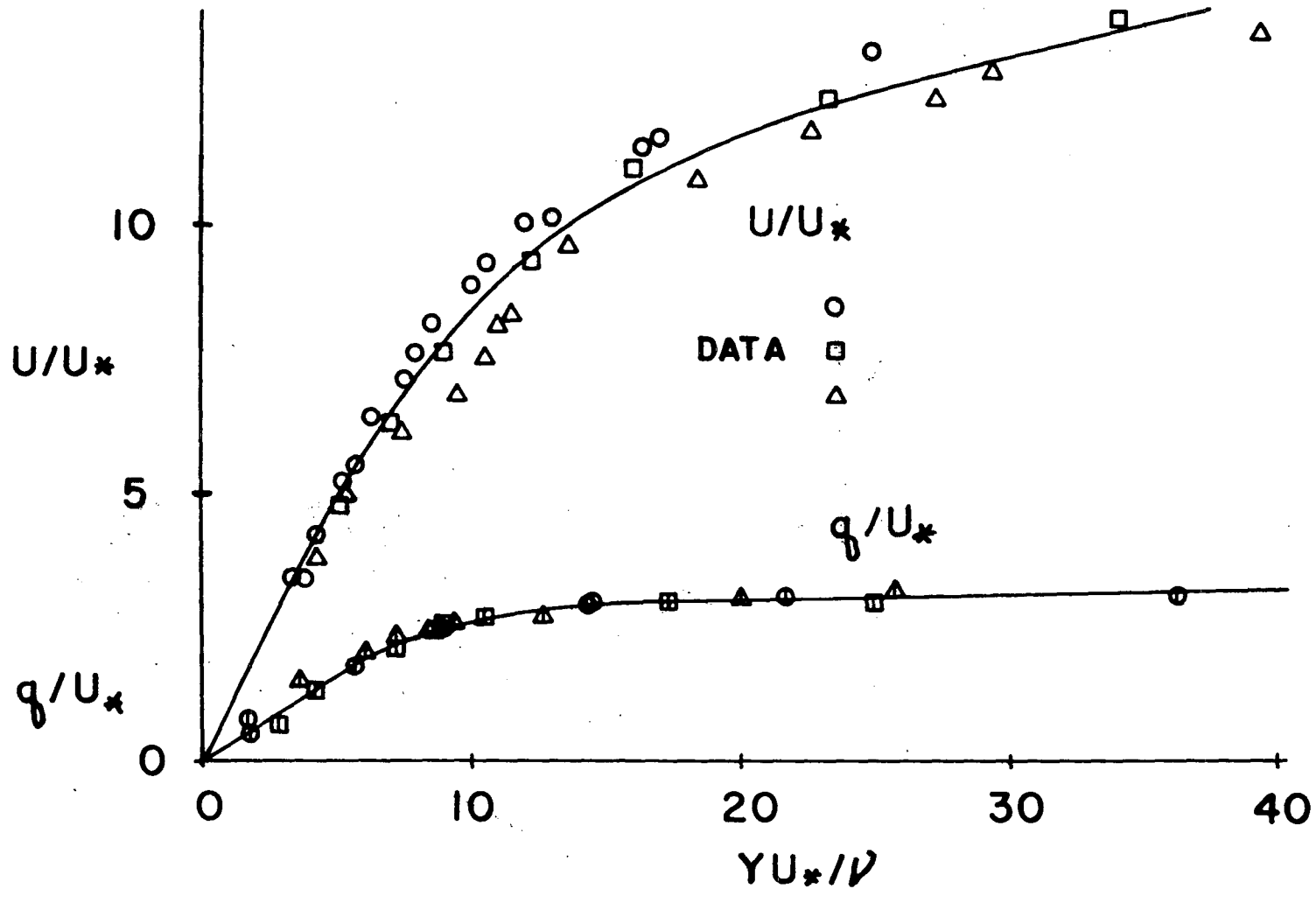

FIG. 17a

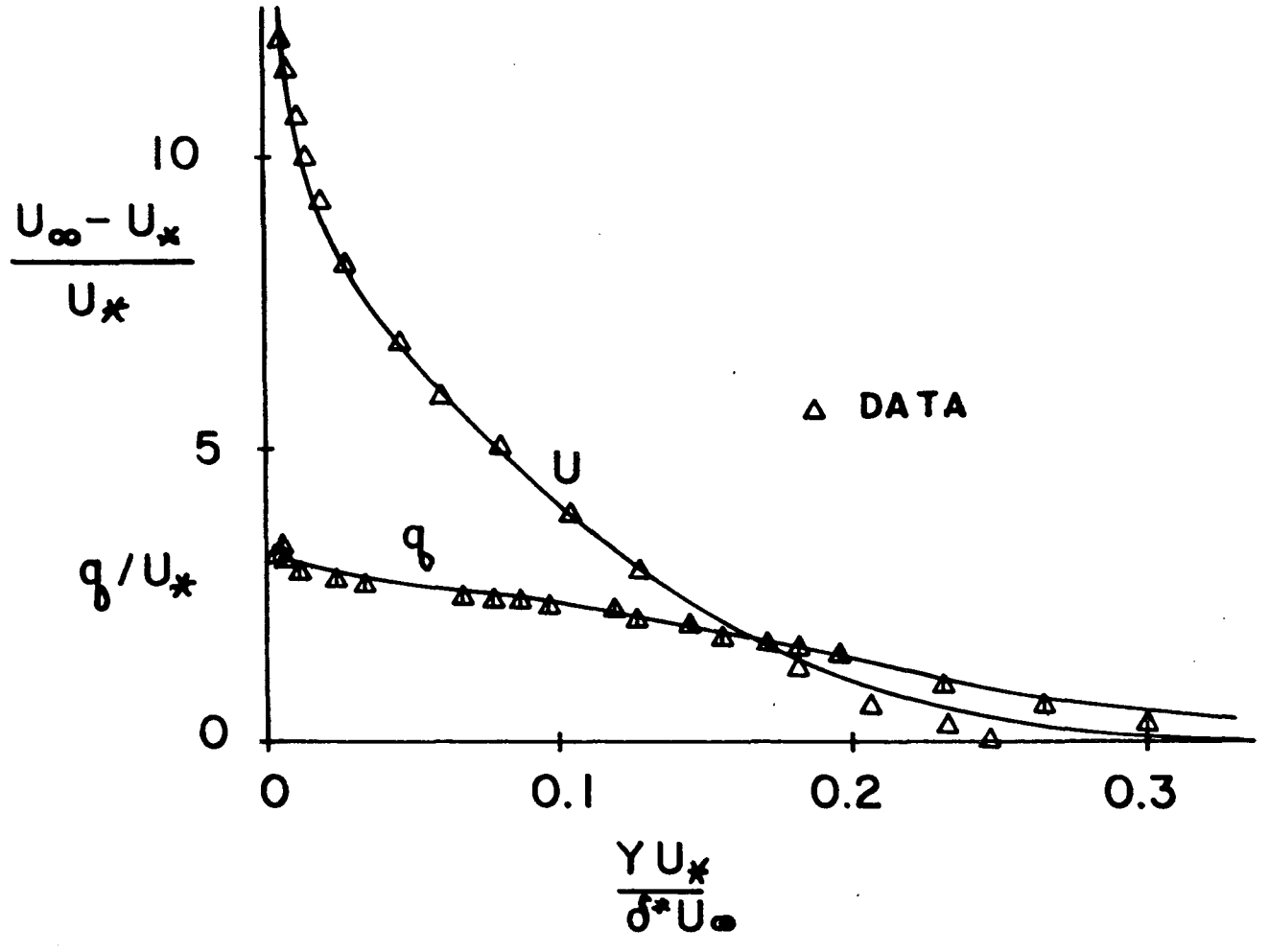

FIG. 17b

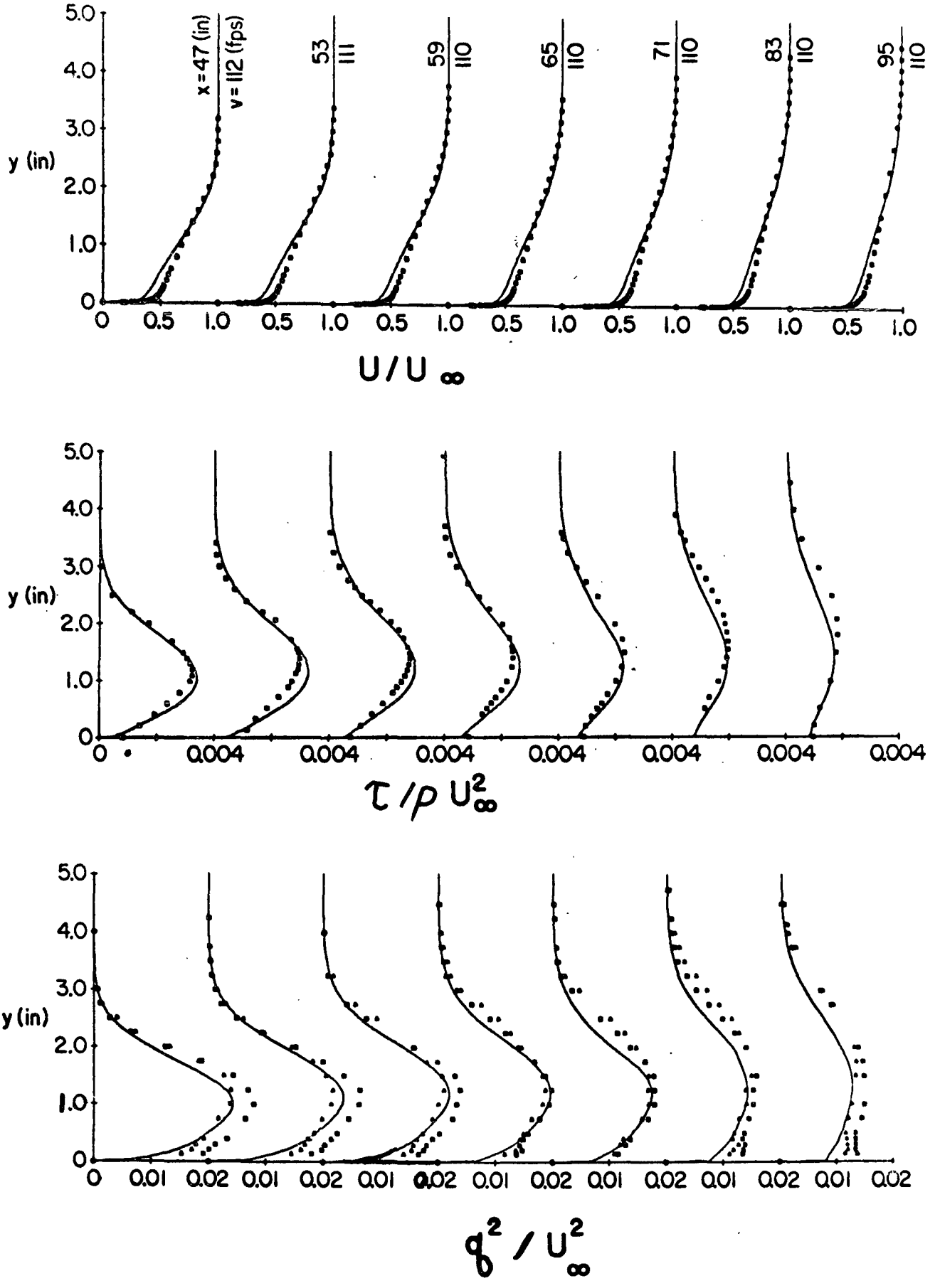
x=47 (in)
v=112 (fps)
53
111
59
110
65
110
71
110
83
110
95
110
y (in)
5.0
4.0
3.0
2.0
1.0
0
0.5
1.0
U/U∞
0.004
τ/ρU∞²
0.01
0.02
q²/U∞²

FIG. 18

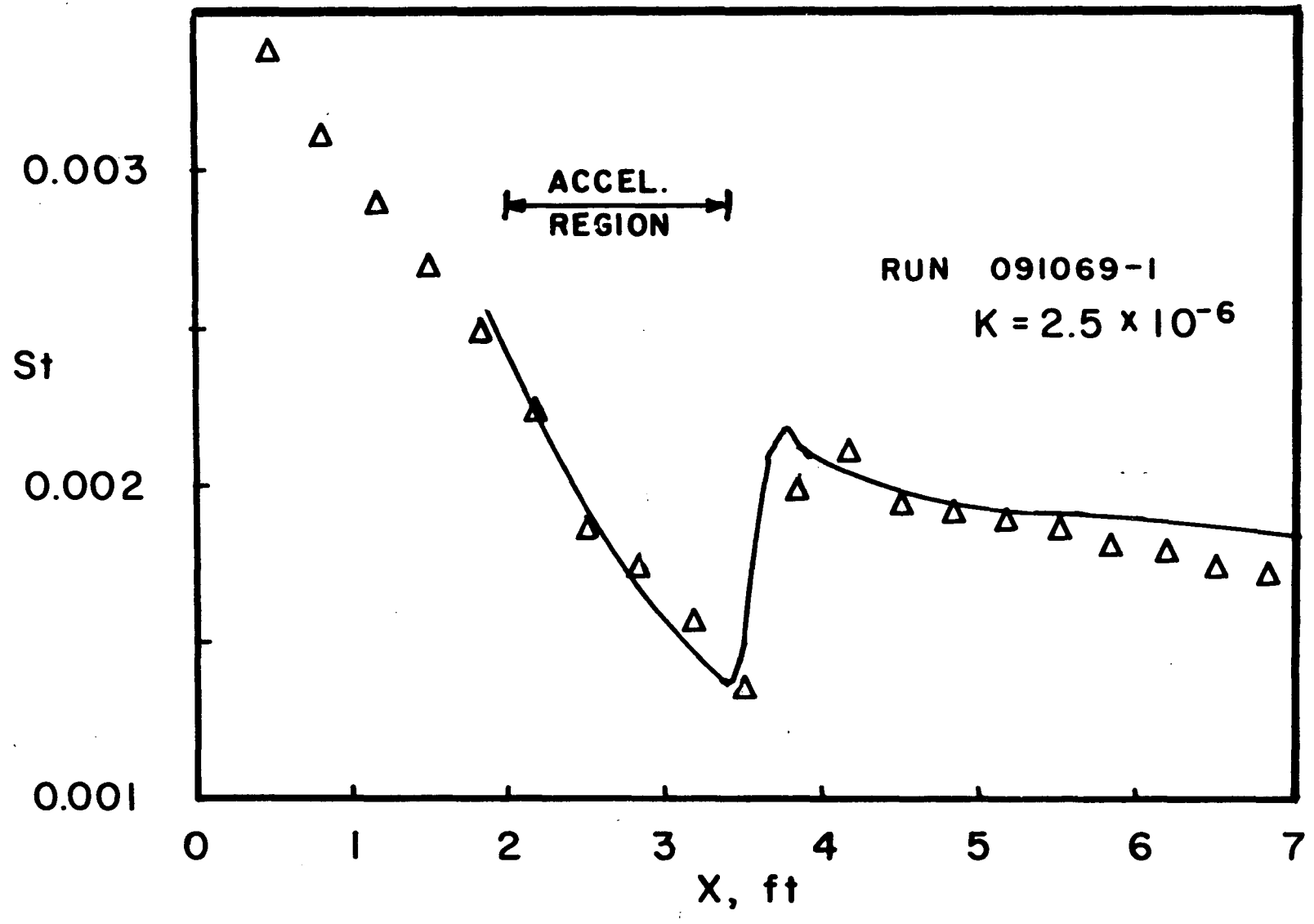
0.003
0.002
0.001
St
ACCEL.
REGION
RUN 091069-1
K = 2.5 x 10⁻⁶
0
1
2
3
4
5
6
7
X, ft

FIG. 19

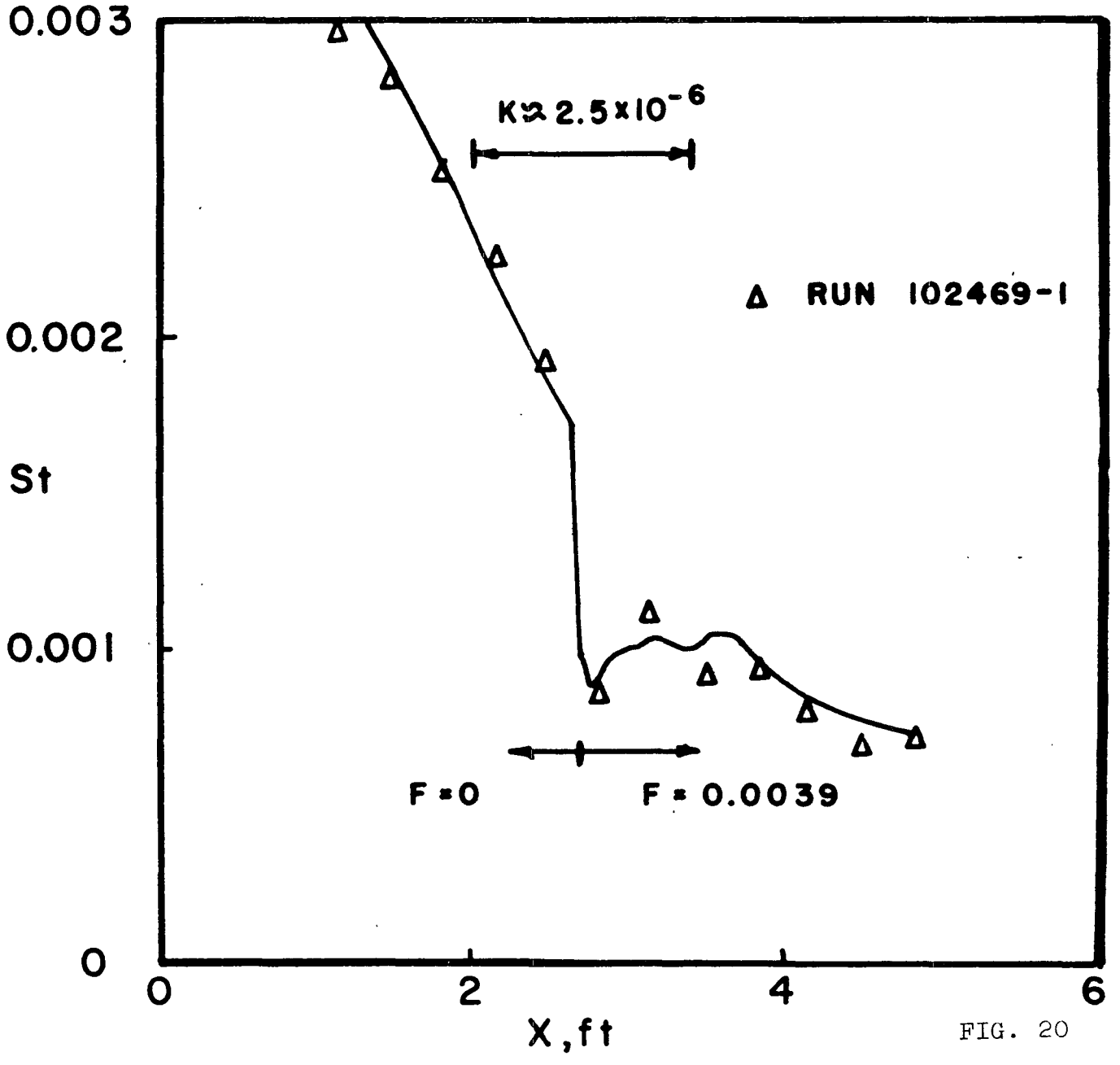

FIG. 20

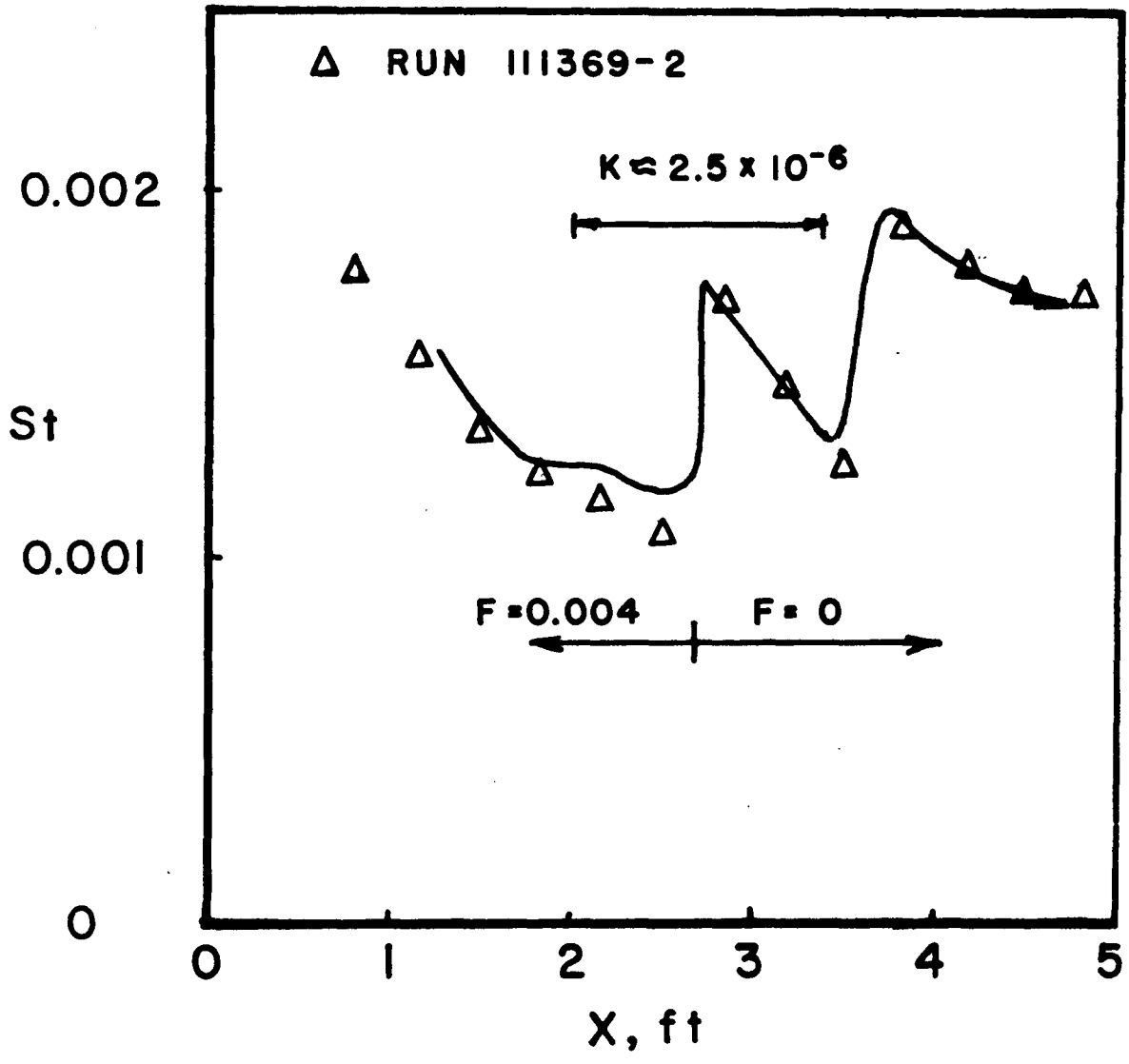

FIG. 21

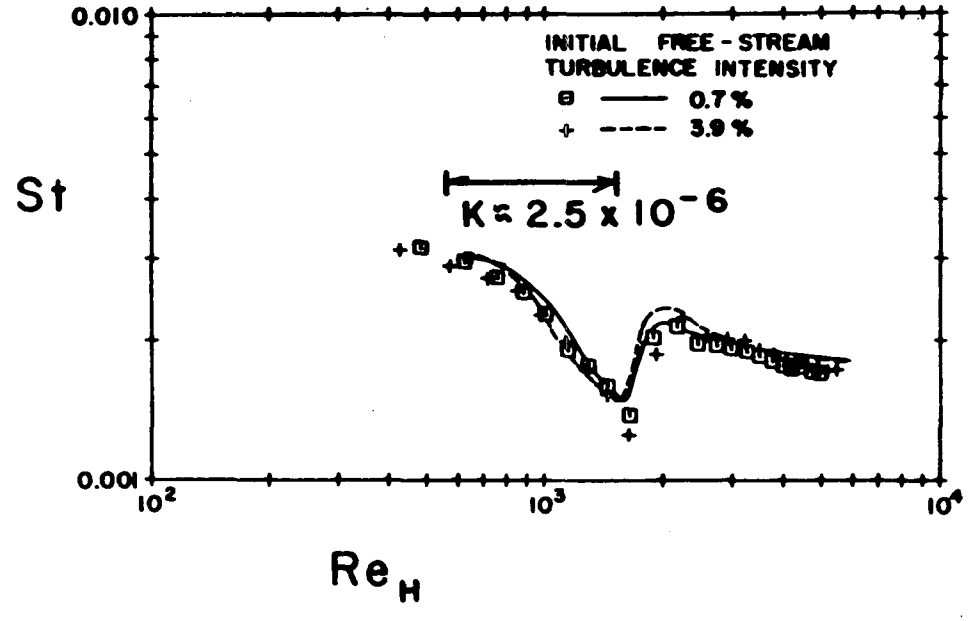
0.010
0.001
St
INITIAL FREE-STREAM
TURBULENCE INTENSITY
0.7%
3.9%
K ≈ 2.5 x 10⁻⁶
10²
10³
10⁴
Re H

FIG. 22

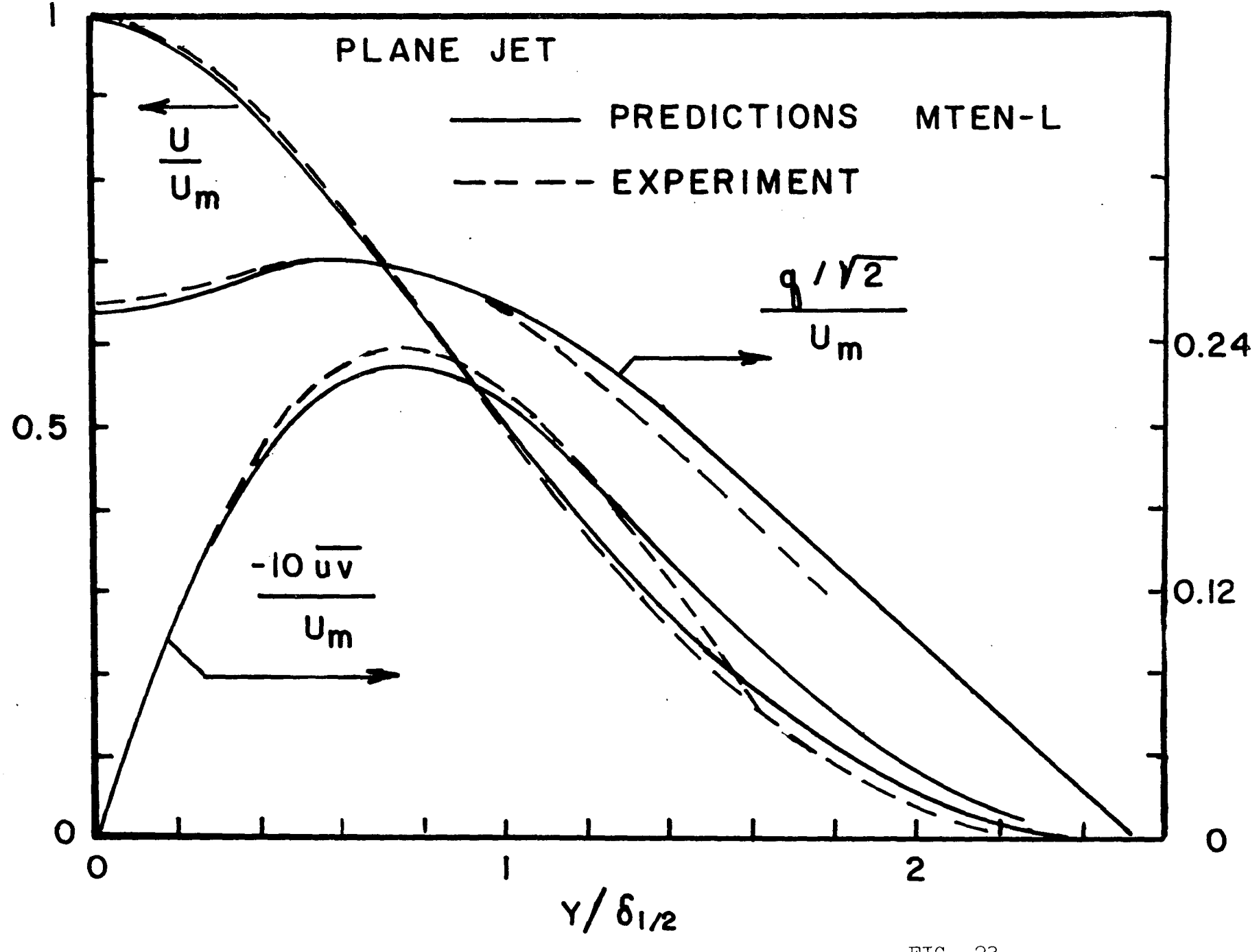
PLANE JET
PREDICTIONS MTEN-L
EXPERIMENT
U/Um
q/√2 / Um
-10 uv / Um
1
0.5
0
0.24
0.12
0
0
1
2
Y/δ1/2

FIG. 23

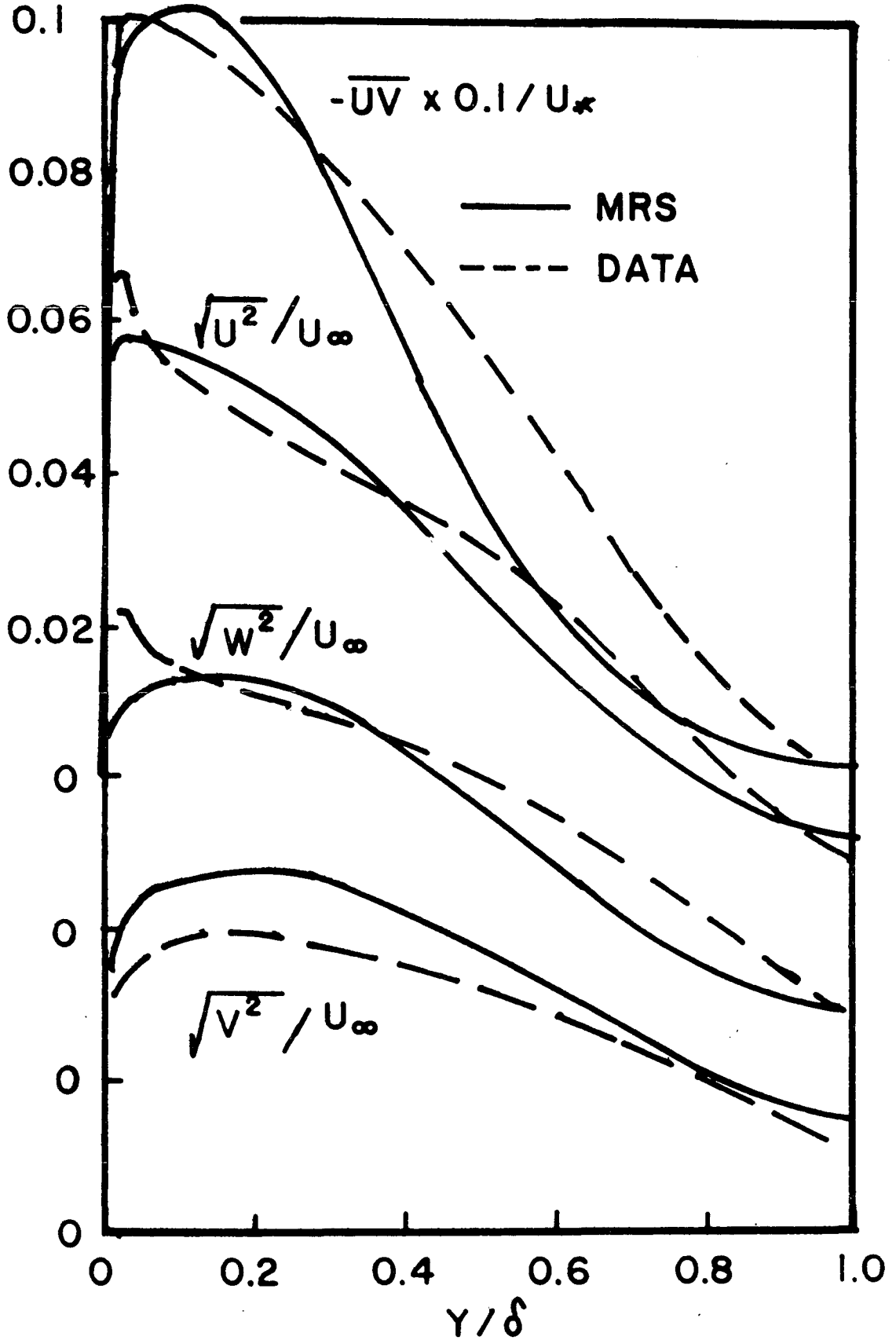
0.1
0.08
0.06
0.04
0.02
0
0
0
0
0
0.2
0.4
0.6
0.8
1.0
Y/δ
$-\overline{UV} \times 0.1 / U_*$
MRS
DATA
$\sqrt{U^2}/U_\infty$
$\sqrt{W^2}/U_\infty$
$\sqrt{V^2}/U_\infty$

FIG. 24

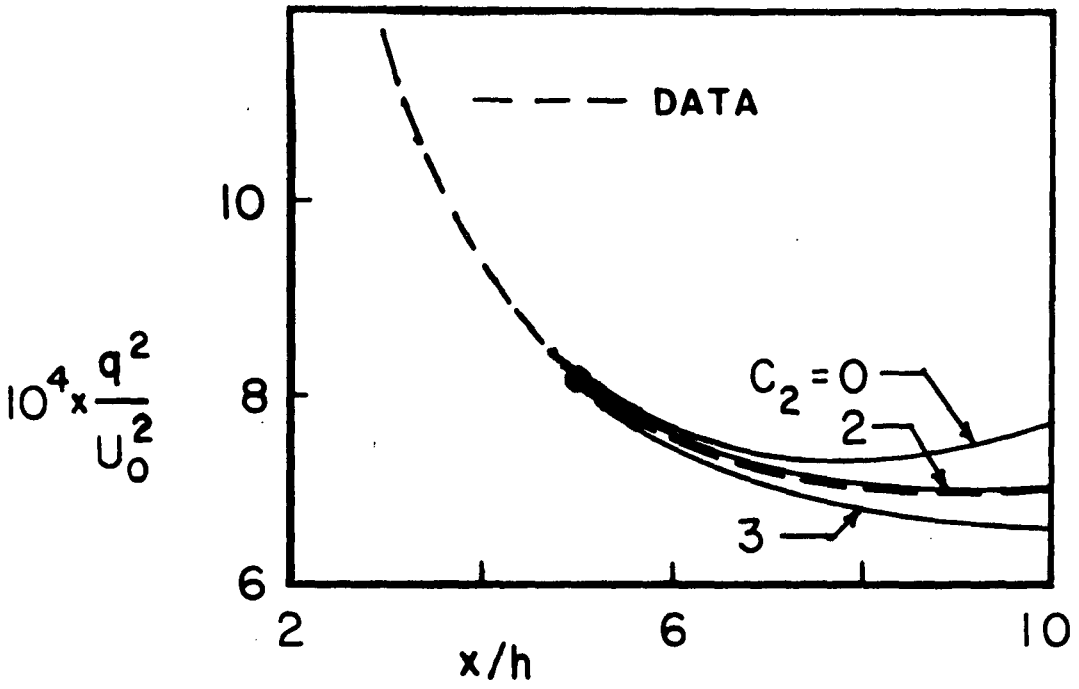
DATA
10
8
6
$10^4 \times \frac{q^2}{U_0^2}$
$C_2 = 0$
2
3
2
6
10
x/h

(a)

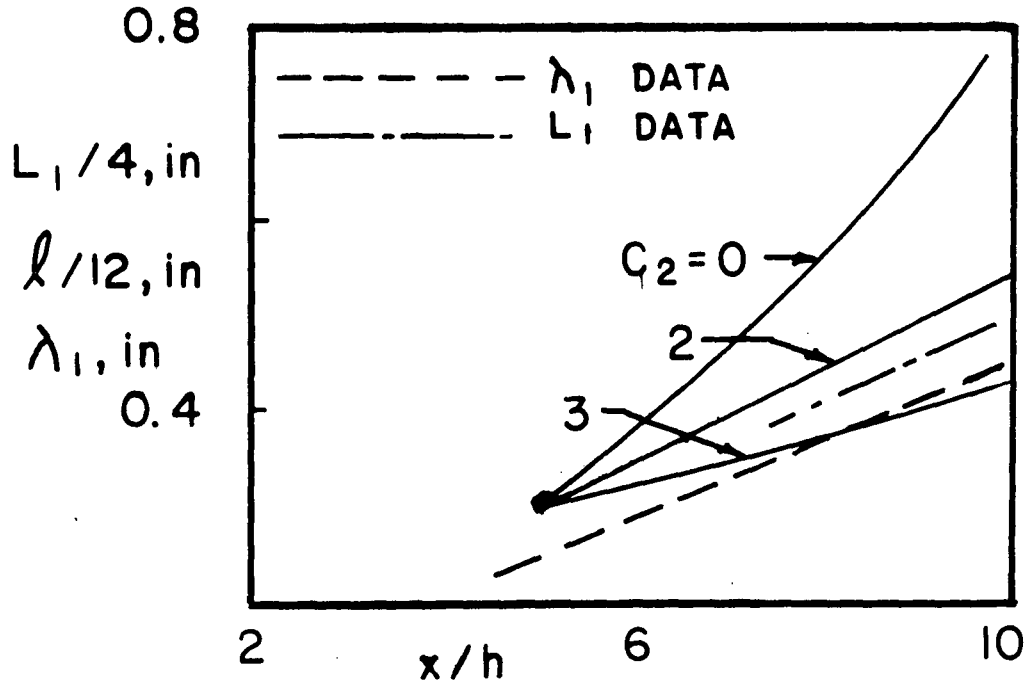
0.8
$L_1/4$, in
$\ell/12$, in
λ_1, in
0.4
λ_1 DATA
L_1 DATA
$C_2 = 0$
2
3
2
6
10
x/h

(b)

FIGS. 25a, b

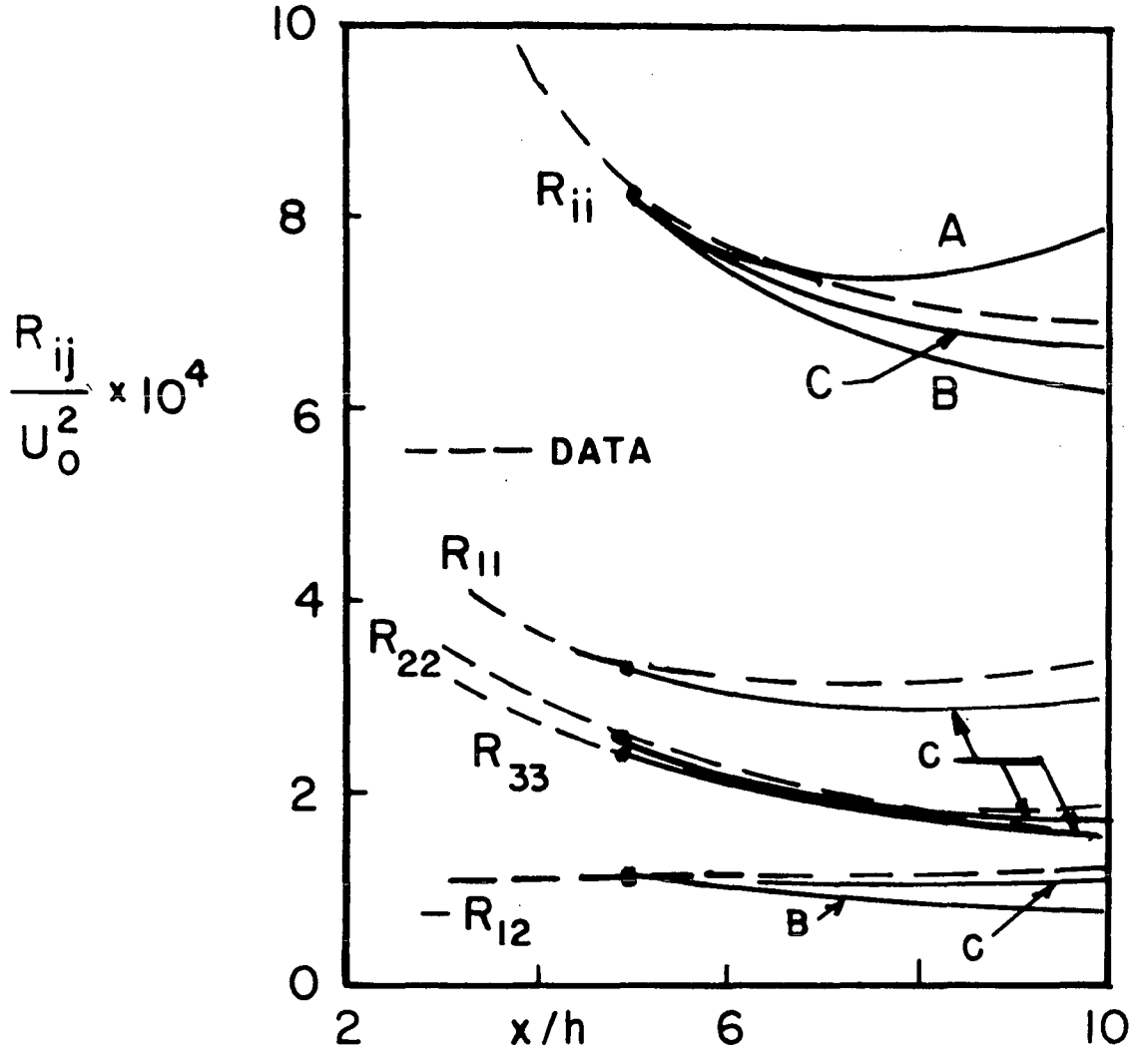
$\frac{R_{ij}}{U_o^2} \times 10^4$
10
8
6
4
2
0
R_{ii}
A
C
B
DATA
R_{11}
R_{22}
R_{33}
C
$-R_{12}$
B
C
2
x/h
6
10

(c)

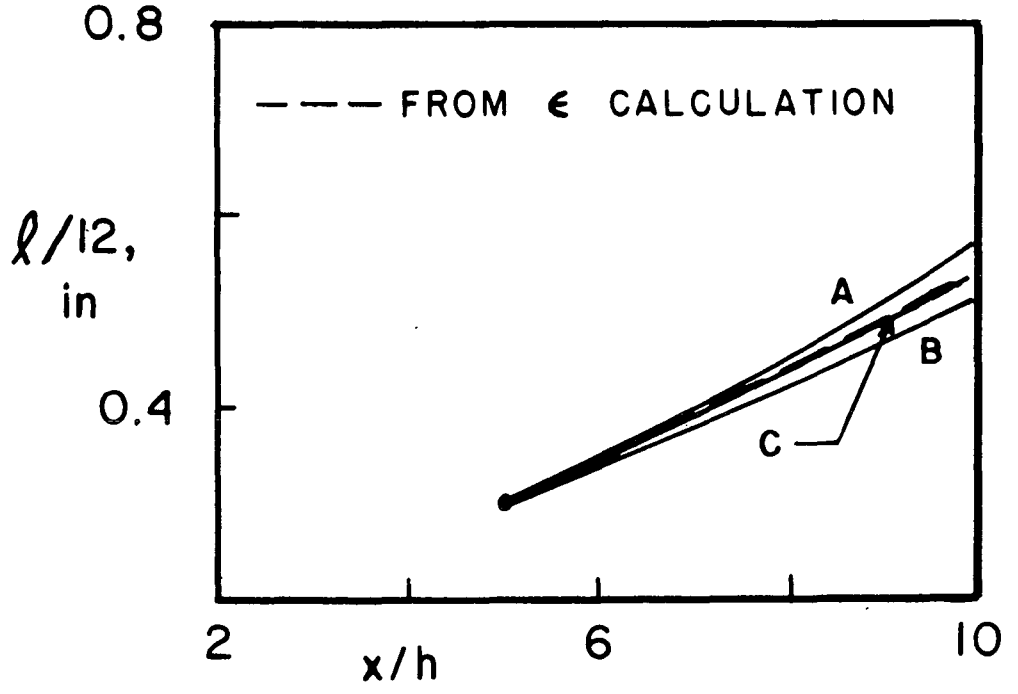
0.8
FROM ϵ CALCULATION
ℓ/12, in
0.4
A
B
C
2
x/h
6
10

(d)

FIGS. 25c, d

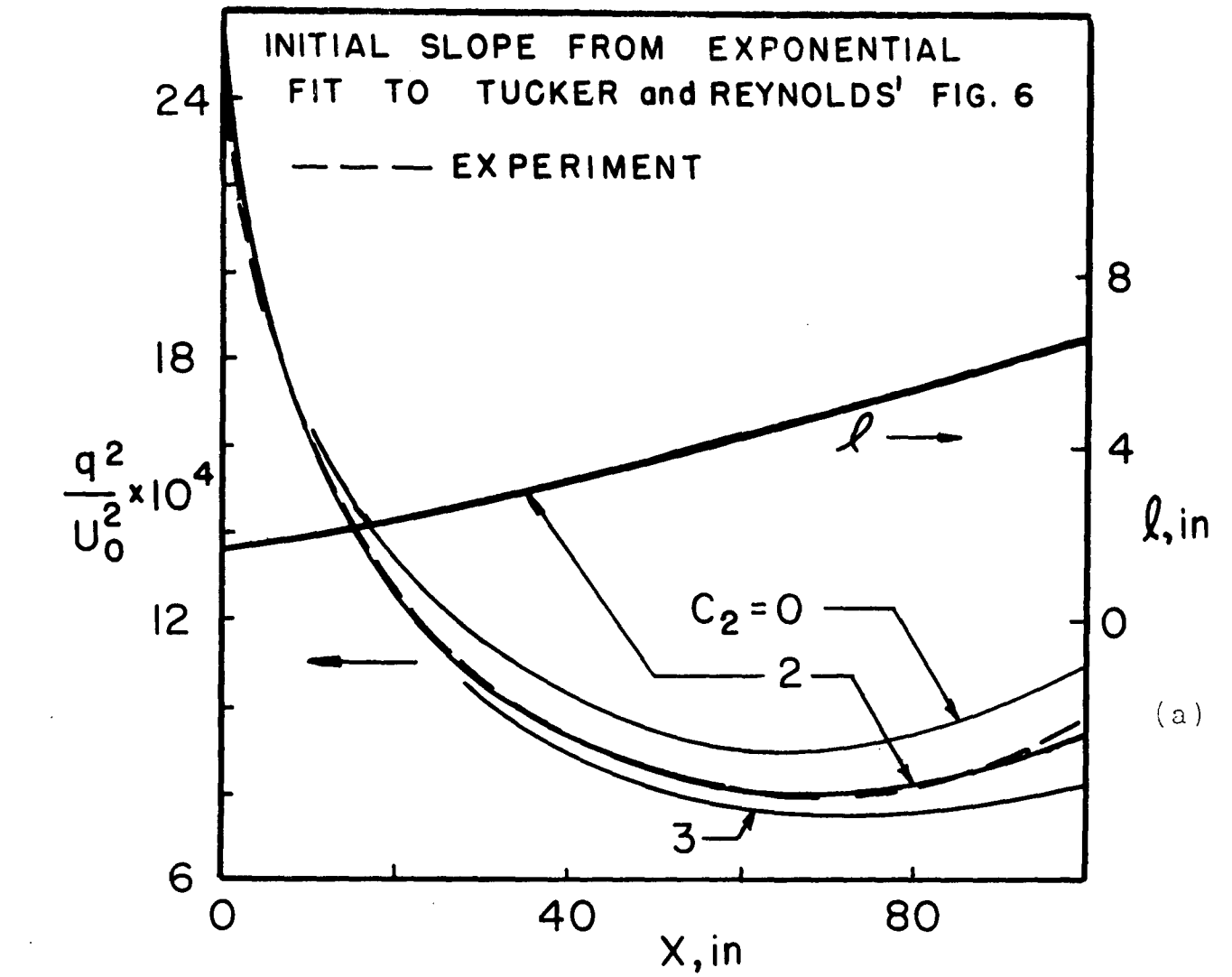
INITIAL SLOPE FROM EXPONENTIAL
FIT TO TUCKER and REYNOLDS' FIG. 6
EXPERIMENT
$\frac{q^2}{U_0^2} \times 10^4$
24
18
12
6
0
40
80
X, in
8
4
0
ℓ, in
ℓ
$C_2 = 0$
2
3

(a)

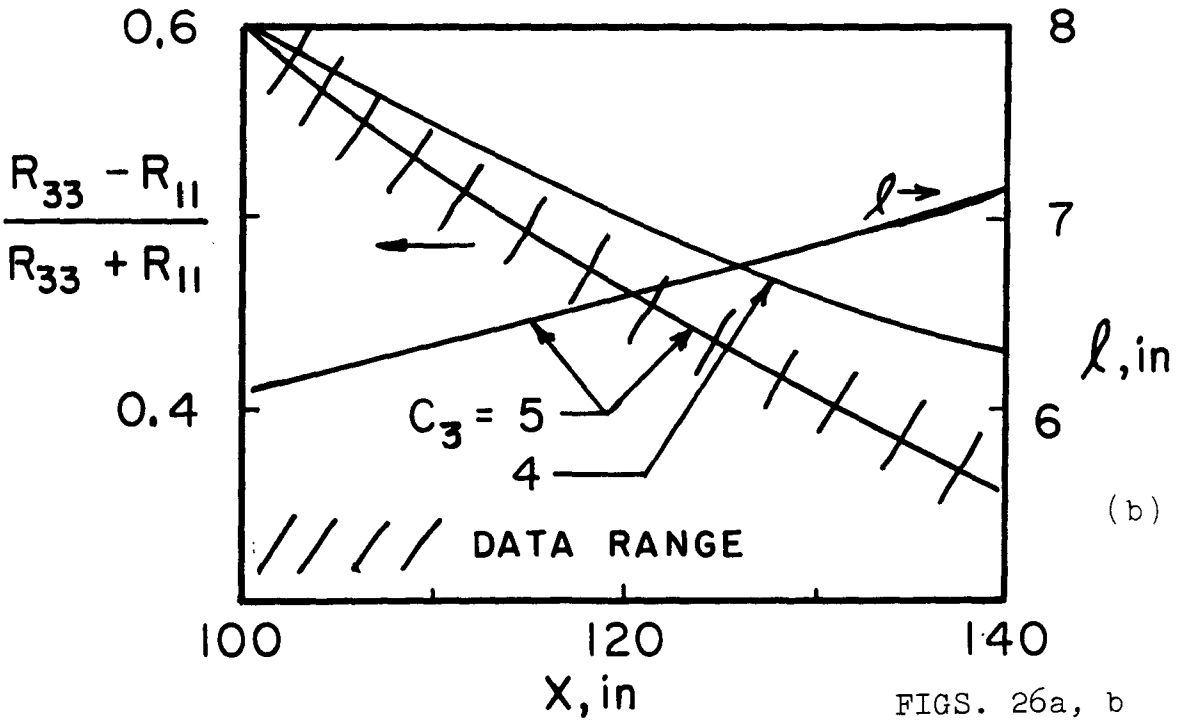
$\frac{R_{33} - R_{11}}{R_{33} + R_{11}}$
0.6
0.4
100
120
140
X, in
8
7
6
ℓ, in
ℓ
$C_3 = 5$
4
DATA RANGE

(b)

FIGS. 26a, b

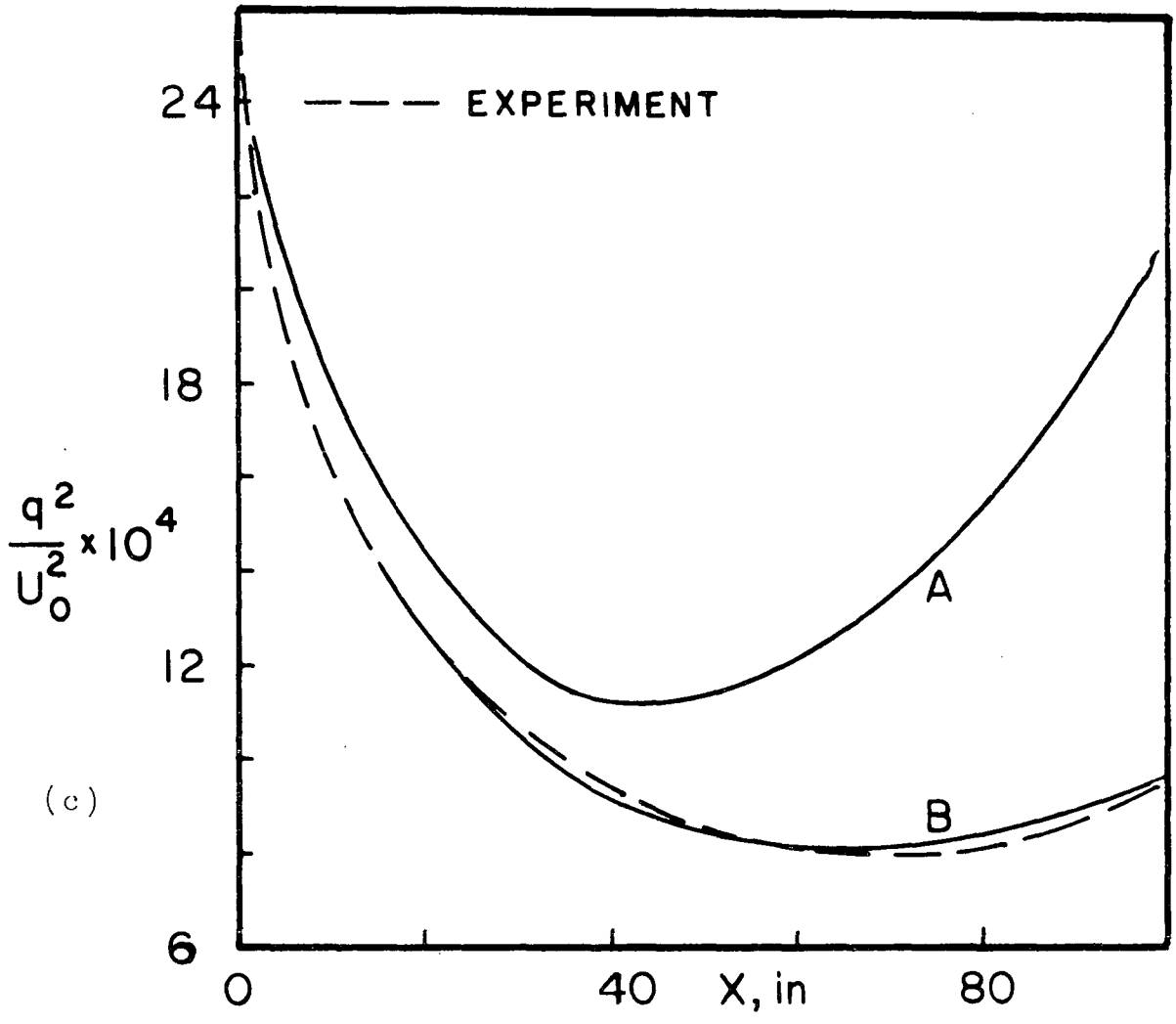
24
18
12
6
EXPERIMENT
$\frac{q^2}{U_o^2} \times 10^4$
A
B
0
40
X, in
80

(c)

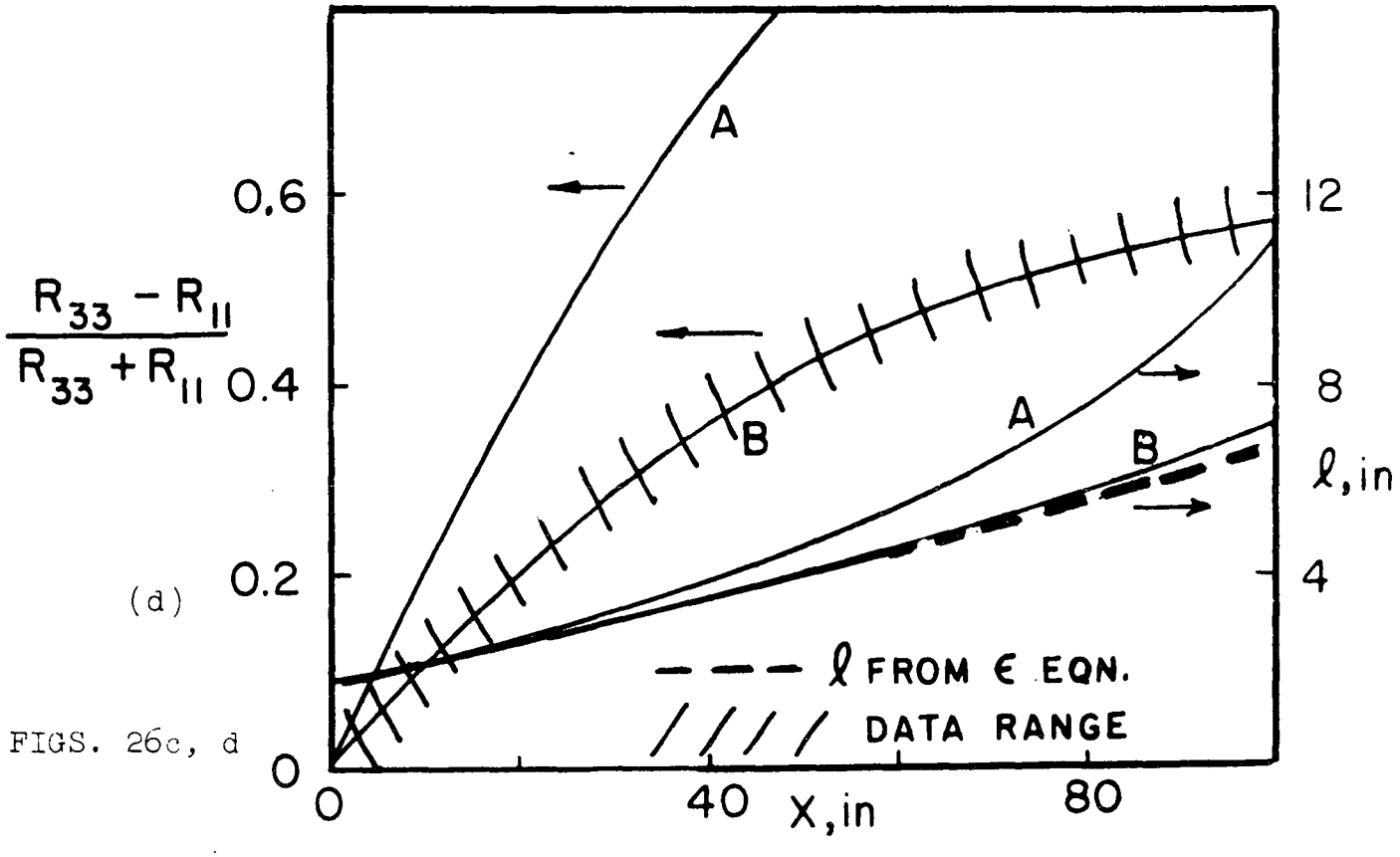
$\frac{R_{33} - R_{11}}{R_{33} + R_{11}}$
0.6
0.4
0.2
0
A
B
A
B
12
8
4
ℓ, in
ℓ FROM ϵ EQN.
DATA RANGE
0
40
X, in
80

(d)

FIGS. 26c, d